
Retrospective Theses and Dissertations

1986

Phase-Locked Loop Based Oscillator Phase Noise Measurement Technique

Luis M. Jimenez
University of Central Florida

 Part of the [Engineering Commons](#)

Find similar works at: <https://stars.library.ucf.edu/rtd>

University of Central Florida Libraries <http://library.ucf.edu>

This Masters Thesis (Open Access) is brought to you for free and open access by STARS. It has been accepted for inclusion in Retrospective Theses and Dissertations by an authorized administrator of STARS. For more information, please contact STARS@ucf.edu.

STARS Citation

Jimenez, Luis M., "Phase-Locked Loop Based Oscillator Phase Noise Measurement Technique" (1986). *Retrospective Theses and Dissertations*. 4980.

<https://stars.library.ucf.edu/rtd/4980>

PHASE-LOCKED LOOP BASED
OSCILLATOR PHASE NOISE MEASUREMENT TECHNIQUE

BY

LUIS MIGUEL JIMENEZ
B.S.E., University of Central Florida, 1984

THESIS

Submitted in partial fulfillment of the requirements
for the degree of Master of Science in the
Graduate Studies Program of the College of Engineering
University of Central Florida
Orlando, Florida

Summer Term
1986

ABSTRACT

Oscillators play an important role in the performance of various radio frequency (RF) systems. The generation of stable carrier and clock frequencies is necessary at both the transmitter and receiver ends of a communication system. Phase noise is the parameter used to characterize an oscillator frequency stability. This thesis introduces a phase noise measurement technique using a phase-locked loop. A 100 MHz Colpitt's oscillator, for the phase noise source, was designed and built. The output of the oscillator was mixed down to 10 MHz, before a phase-locked loop extracted the phase noise information. Measurements were taken and compared to measurements taken at RF frequencies using an HP spectrum analyzer.

Finally, a feedback phase noise model was derived, such that oscillators can be designed with phase noise being a design parameter.

ACKNOWLEDGEMENTS

I would like to acknowledge and thank the people who have contributed to the thesis. First, I would like to dedicate it to my parents for their love and support through the years.

I would like to express my appreciation to the members of my committee for their corrections and time spent evaluating the thesis. Special thanks to my advisor, Dr. M. Belkerdid, whose help and suggestions were crucial to the development of the thesis.

I would also like to express my gratitude to Carl Bishop, Jeff Abbott, and Gary Morrissette for their contributions.

Finally, a special thank you to my wife, Charlotte, for her patience and understanding.

TABLE OF CONTENTS

LIST OF FIGURES	vi
Chapter	
I. INTRODUCTION	1
II. NOISE IN AN OSCILLATING SIGNAL	3
An ideal oscillating signal	3
Real oscillating signals	4
Components of frequency stability	6
Definitions	7
III. REPRESENTATIONS OF PHASE NOISE IN THE FREQUENCY DOMAIN: SPECTRAL DENSITIES	9
Phase and power spectral densities	9
Fractional frequency fluctuations	10
Spectral density of frequency fluctuations	12
Spectral density of fractional frequency fluctuations	12
$\hat{f}(f)$ spectral density	12
Relation between $\hat{f}(f)$ and S_{ϕ}	13
IV. PHASE NOISE MEASUREMENTS	16
Importance of phase noise measurements	16
Random noise corrections	18
Measurement techniques	20
V. 100 MHz OSCILLATOR DESIGN	23
Oscillator Analysis	23
Oscillator design	29
Results	33
VI. PLL MEASUREMENT TECHNIQUE DESIGN AND IMPLEMENTATION	37
System design	37
Mathematical analysis	42
Calibration	45
Measurements and results	48

VII. A FEEDBACK MODEL FOR OSCILLATOR PHASE NOISE . . .	53
Noise in amplifiers	53
Feedback model of phase noise	57
Phase noise design considerations	59
VIII. CONCLUSION	62
Appendices	
A. OSCILLATOR DESIGN FORMULAS	64
B. PROGRAMS LISTINGS	67
C. AUTOMATED PHASE NOISE SYSTEMS	70
REFERENCES	74

LIST OF FIGURES

1. Ideal oscillating signal	4
2. Components of frequency	5
3. $\phi(f_m)$ definition	13
4. Effect of high level sidebands	17
5. Phase noise effect on a QPSK system	17
6. Frequency discriminator system	22
7. Phase quadrature system	22
8. Colpitt's oscillator	24
9. Equivalent transistor model	25
10. Equivalent oscillator model	25
11. Colpitt's tank circuit	28
12. Colpitt's ideal transformer equivalent	28
13. Oscillator equivalent output circuit	30
14. Oscillator DC circuit	32
15. Colpitt's final circuit configuration	34
16. Time domain output	35
17. Frequency domain output	36
18. Phase noise measurement system	37
19. Normalized third-order Butterworth	38

20. LPF magnitude response	39
21. PLL circuit schematic	40
22. Local oscillator spectrum	43
23. Oscillator spectrum	44
24. Calibration system	46
25. RF phase noise spectrum result	50
26. Audio spectrum of demodulated output	51
27. PLL measurement result	52
28. Amplifier noise spectrum	54
29. Model for a noise free amplifier	55
30. Phase deviation at $f_o + f_m$	55
31. Amplifier phase noise model	56
32. Phase noise feedback model	59
33. Power-law processes of oscillator phase noise.	60

CHAPTER ONE
INTRODUCTION

The increasing use of the electromagnetic spectrum requires the need for very accurate and stable frequencies. Phase noise is the term used to describe frequency stability. It is because of this phase noise that many microwave and RF systems offer a limited performance. Poor resolution in radar, interference in communications, and bit error rate degradation in phase modulated systems are some of the results of high levels of phase noise. Nevertheless, phase noise is a term sometimes misunderstood due to the light coverage of the subject in most engineering books. For information on the phase noise concept one must resort to the specialized literature such as Hewlett-Packard application notes, National Bureau of Standards technical notes, and IEEE publications.

Phase noise will be introduced in this paper by starting with the basic concepts of an oscillator signal, such as the phase-frequency relationship, by characterizing the components of stability, and by its definition. Since phase noise is represented in the frequency domain as a

spectral density, four different but related spectral densities will then be developed.

Random noise measurements require some corrections that are not necessary for deterministic signals; these corrections will be explained. Next, the three most common phase noise measurement techniques will be introduced. These techniques are: Direct RF Spectrum measurement, Frequency Discriminator, and Phase Quadrature Detection.

Before measurements can be made a source of phase noise, an oscillator, is needed. For this purpose a 100 MHz Colpitt's oscillator will be designed in a step-by-step, detailed manner. This oscillator output will be mixed down in frequency so that a phase-locked loop extracts the phase noise information. This new phase noise measuring method will be introduced in this thesis along with the required calibration of the system used. The results will be compared to measurements taken using the direct RF technique.

A key element in the design of clean oscillators is the Q factor of the resonator circuit. A feedback phase noise model will be derived from which a relationship for Q will be obtained. This will give the designer a phase noise parameter to be used in the design of oscillators.

CHAPTER TWO
NOISE IN AN OSCILLATING SIGNAL

An Ideal Oscillating Signal

An ideal oscillating signal can be represented by the sine wave shown in Figure 1.

The period "T" is the time it takes to complete one oscillation cycle. The frequency "f" is the reciprocal of the period, or the number of cycles per second. The phase "φ" is the angle within a cycle corresponding to a time "t," and it is given in radians by

$$\phi = 2\pi \frac{t}{T}$$

which can be written as

$$\phi = 2\pi ft$$

$$\phi = \omega t \tag{2.1}$$

The voltage "V" is given by

$$V(t) = v_p \sin 2\pi ft \tag{2.2}$$

From Figure 1, and equation (2.1)

$$\frac{\Delta\phi}{\Delta t} = \omega$$

that is, for a given $\Delta\phi$ and Δt there is a sine wave with a unique frequency "w" (in radians per second).

In the limit as $\Delta t \rightarrow 0$

$$\frac{d\phi}{dt} = \omega_i \quad (2.3)$$

This relationship defines the instantaneous frequency as the time derivative of the phase.

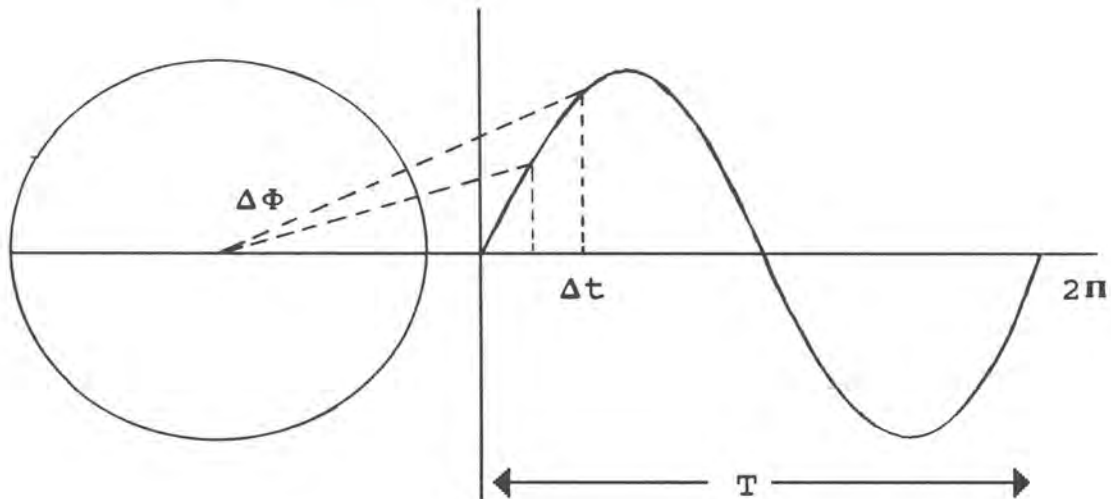


Figure 1. Ideal oscillating signal.

Real Oscillating Signals

An ideal oscillator produces a pure sine wave carrier having a fixed frequency, constant phase, and constant amplitude. Oscillators used in practice, however, are non ideal and contain frequency instabilities and phase and amplitude noise.

The instantaneous frequency of an oscillator can be considered to have three basic components: a constant or designed value (ω_c), a randomly varying frequency ($\omega_r(t)$),

and a slowly varying drift component (αt). These components are shown on Figure 2. All these frequency deviations from the nominal or designed frequency are undesirable and are considered noise. To account for the noise components, equation (2.2) will have to be modified

$$V(t) = [v_0 + e(t)] \sin[2\pi f_0 t + \phi(t)] \quad (2.4)$$

where

v_0 = nominal peak amplitude

$e(t)$ = amplitude noise

f_0 = nominal frequency

$\phi(t)$ = phase noise

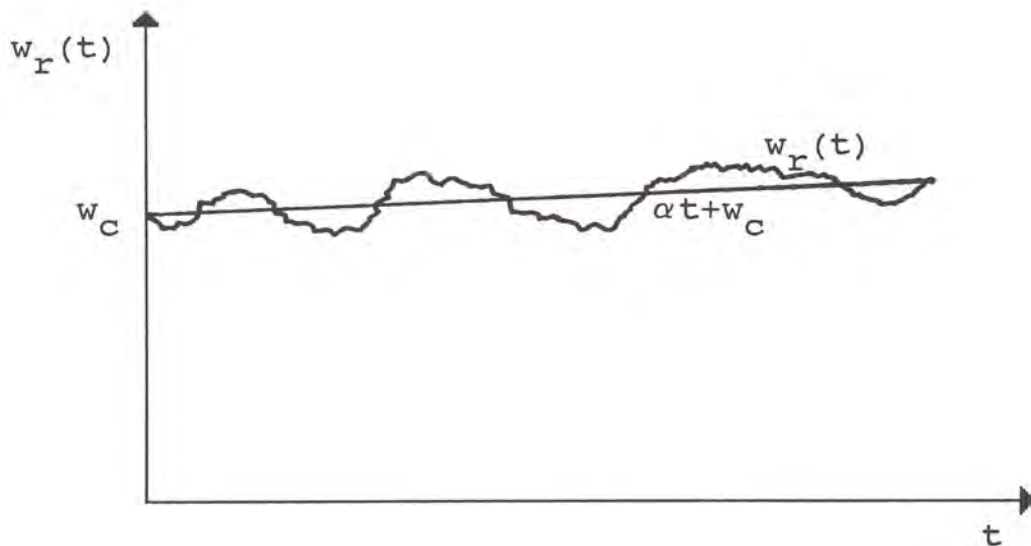


Figure 2. Components of frequency.

Components of Frequency Stability

From the previous section, and working towards a definition of phase noise, it is clear that it would be advantageous to characterize three components of stability.

The first component includes those frequency shifts due to changes in the environment such as temperature, pressure, and gravity. The second component includes those slow changes in frequency, such as those due to aging. This is called long-term stability, and it is expressed in parts per million of frequency change per hour, day, month, or year. These two components are important in certain applications, but with proper design, such as a feedback loop to correct for the slow drift in frequency, or the use of compensating capacitors for the temperature changes, most of these effects can be eliminated or minimized. The third component includes those elements that cause frequency noise and fluctuations with random periods shorter than a few seconds. This is called short-term stability, and it is going to be the focus of this paper.

Short-term stability is the one that causes the worst problems. If the oscillator rapidly changes its output level up and down some sidebands representing amplitude modulation will appear. If the oscillating signal shifts back and forth rapidly in frequency, the resulting phase modulation will also produce sidebands. The more important components

are the phase modulating signals since amplitude noise is often reduced significantly by limiting, and its absence is a good approximation applied to oscillator design and modeling.

Definitions

Two types of signals can be clearly distinguished. Deterministic signals, which show up as distinct components in a spectral plot, can be related to known factors such as power line frequency. Random signals which include noise such as thermal, shot, and flicker. Phase noise is the name given to this "randomly generated phase modulating signals," and is the main factor affecting the short-term stability.

In addition to the short term random phase noise, a term used to characterize the frequency fluctuations of an oscillator is the frequency stability which is defined (Howe 1976) as "the degree to which an oscillating signal produces the same value of frequency for any interval, Δt , throughout a specified period of time."

From the above definitions the same problem, that of noise in an oscillator, receives two different names depending on the oscillator application. If the application involves characterizing the structure of the spectrum created by the randomly generated phase modulating signals, such as in sources of carriers in radar and communication

signals, then the term used is phase noise. If the application involves sources of timing and synchronizing signals, then the term used is frequency stability.

Phase noise, being the topic of this paper, will be characterized by its output spectrum.

CHAPTER THREE

REPRESENTATION OF PHASE NOISE IN THE FREQUENCY DOMAIN: SPECTRAL DENSITIES

Since noise can be characterized by means of spectrum analysis, stabilities in the frequency domain are usually specified as spectral densities. Four different, but related, types of spectral densities will be introduced in this chapter.

Phase and Power Spectral Densities

When power is plotted versus frequency the result is the power spectrum. If this power spectrum is normalized as to make the total area under the curve equal one, then it is called the power spectral density. This power spectrum, or RF spectrum, can be separated into two different and independent spectra. One is the AM power spectral density, which is the result of fluctuations in " $e(t)$," and the other is the spectral density of fluctuations in " $\phi(t)$." The AM power spectral density is usually negligible, and if we assume that the modulation of the phase fluctuations is small, the RF spectrum has approximately the same shape as the phase spectral density with two main differences.

The phase spectral density does not include the fundamental carrier. If the carrier is considered as DC, the frequencies measured with respect to the carrier are referred to as offset from the carrier, or Fourier frequencies. They will be designated as f_m .

The phase fluctuations in the time domain are given by $\phi(t)$ which in the frequency domain corresponds to $\phi(f)$. The spectral density of phase fluctuations is, then, given by

$$S_\phi(f) = \phi^2(f)_{\text{rms}} \quad (3.1)$$

and has units of $\frac{\text{rad}^2}{\text{Hz}}$ instead of $\frac{\text{watts}}{\text{Hz}}$

From 3.1 the second moment of phase noise, $\overline{\phi^2(t)}$, is obtained by integrating $S_\phi(f)$. This can be shown using the Weiner-Khintchine theorem that states that the autocorrelation function $R_\phi(\tau)$ and the spectral density function $S_\phi(f)$ of a random variable form a Fourier transform pair.

The total power is given by $R_\phi(\tau)$ when $\tau = 0$, that is

$$\begin{aligned} R_\phi(\tau) &= \int_{-\infty}^{\infty} e^{j\omega\tau} S_\phi(f) df \\ R_\phi(0) &= \int_{-\infty}^{\infty} S_\phi(f) df \end{aligned} \quad (3.2)$$

The autocorrelation function is defined as

$$R_\phi(\tau) = \lim_{T \rightarrow \infty} \frac{1}{T} \int_{-\frac{T}{2}}^{\frac{T}{2}} \phi(t)\phi(t+\tau) dt$$

$$R_{\phi}(0) = \lim_{T \rightarrow \infty} \frac{1}{T} \int_{-\frac{T}{2}}^{\frac{T}{2}} \phi^2(t) dt = \overline{\phi^2(t)} \quad (3.3)$$

Combining equations 3.2 and 3.3

$$\overline{\phi^2(t)} = \int_{-\infty}^{\infty} S_{\phi}(f) df$$

Fractional Frequency Fluctuations

Equation 2.3 says that frequency is equal to the rate of change in phase. That is, fluctuations in frequency are related to phase fluctuations since the rate of $\phi(t)$ must be changed to accomplish a shift in $f(t)$.

From equations 2.3 and 2.4

$$\frac{d\phi}{dt} = 2\pi f_0 + \frac{d\phi(t)}{dt}$$

$$\frac{d\phi}{dt} = 2\pi f(t)$$

$$2\pi f(t) = 2\pi f_0 + \frac{d\phi(t)}{dt}$$

$$\frac{d\phi(t)}{dt} = 2\pi f(t) - 2\pi f_0$$

let $f(t) - f_0 = \Delta f(t)$

$$\Delta f(t) = \frac{1}{2\pi} \frac{d\phi(t)}{dt} \quad (3.4)$$

$\Delta f(t)$ is called the frequency fluctuation. Dividing both sides by f_0 (the carrier frequency) equation 3.4 becomes

$$\frac{\Delta f(t)}{f_0} = \frac{1}{2\pi f_0} \frac{d\phi(t)}{dt} \quad (3.5)$$

The term $\frac{\Delta f(t)}{f_0}$ is dimensionless, and is called

the fractional frequency fluctuation. The purpose of this normalization is to generate a frequency stability figure of merit. Two oscillators operating at different frequencies could have the same frequency fluctuation, but the higher the operating frequency the smaller the fractional frequency fluctuation which implies a higher figure of merit.

Spectral Density of Frequency Fluctuations

From equation 3.4, and using the differentiation property of the Fourier transforms

$$\Delta f(f) = \frac{2\pi f}{2\pi} \phi(f)$$

$$S_{\Delta f}(f) = f^2 S_{\phi}(f) \quad \left| \frac{\text{Hz}^2}{\text{Hz}} \right| \quad (3.6)$$

Spectral Density of Fractional Frequency Fluctuations

From equation 3.5, and letting $\frac{\Delta f(t)}{f_0} = y$

$$y(f) = \frac{2\pi f}{2\pi f_0} \phi(f)$$

$$S_Y(f) = \frac{f^2}{f_0^2} S_\phi(f) \quad | \text{ Hz}^{-1} | \quad (3.7)$$

$\epsilon(f)$ Spectral Density

The spectral density of the randomly phase modulating signal is not, in many cases, what is of interest but rather the sideband power of the phase noise with respect to the carrier level. This indirect representation of phase noise is the spectral density specified by the symbol $\epsilon(f_m)$

$$\epsilon(f_m) = \frac{\text{Pssb (per 1 Hz)}}{\text{Ps}} \quad \left| \frac{\text{dBc}}{\text{Hz}} \right| \quad (3.8)$$

which is defined (Scherer 1986) "as the ratio of the single sideband noise power in a 1 Hz bandwidth to the total carrier power specified at a given offset frequency (f_m) of the carrier." See Figure 3.

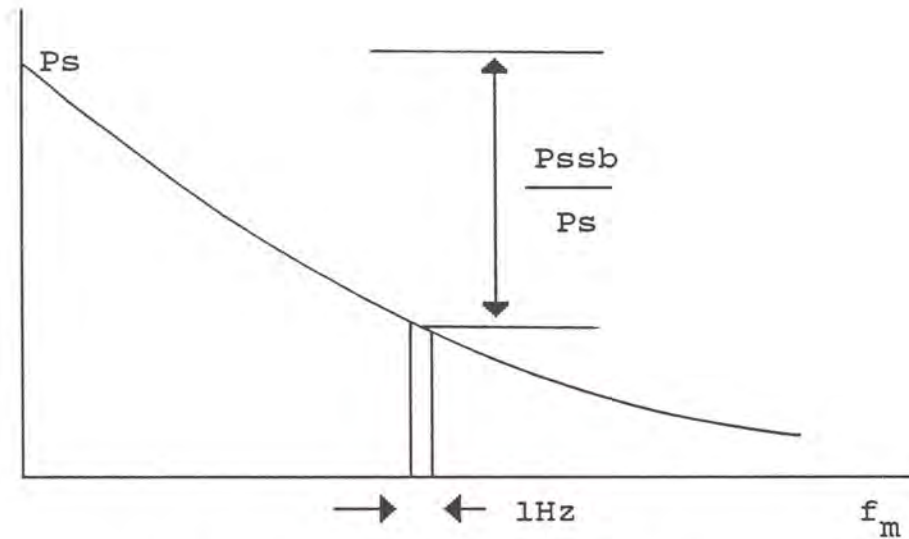


Figure 3. $f(f_m)$ Definition.

Relation Between $f(f)$ and $S\phi(f)$

From angle modulation theory, a phase modulated signal is given by

$$V(t) = A \cos(\omega_c t + \phi_p \sin \omega_m t) \quad (3.9)$$

where ϕ_p is the peak phase deviation equivalent to the modulation index (β) for sinusoidal modulation.

Equation 3.9 can be written as

$$V(t) = A \text{ real } [e^{j\omega_c t} e^{j\beta \sin \omega_m t}] \quad (3.9a)$$

For narrowband modulation, that is $\beta \ll 1$

$$e^{j\beta \sin \omega_m t} \approx 1 + j\beta \sin \omega_m t$$

Equation 3.9a can then be rewritten as

$$V(t) = A \text{ real } \{(\cos \omega_c t + j \sin \omega_c t) (1 + j\beta \sin \omega_m t)\}$$

$$V(t) = A \cos \omega_c t - \beta A \sin \omega_c t \sin \omega_m t$$

with the aid of a trigonometric identity

$$V(t) = A \cos w_c t - \frac{\beta A}{2} \cos (w_c - w_m)t + \frac{\beta A}{2} \cos (w_c + w_m)t$$

which implies that

$$J_0(\beta) = A, \quad J_1(\beta) = \frac{\beta A}{2}, \quad J_{-1}(\beta) = \frac{\beta A}{2}$$

that is, for small β

$$\frac{J_1(\beta)}{J_0(\beta)} = \frac{\beta}{2}$$

From the definition of $\epsilon(f)$

$$\epsilon(f) = \frac{J_1^2}{J_0^2} = \left(\frac{\beta}{2}\right)^2 = \frac{1}{4} \phi_p^2 = \frac{1}{4} (2 \phi_{rms})^2 = \frac{1}{2} (\phi_{rms})^2$$

$$\epsilon(f) = \frac{1}{2} S_\phi(f) \quad (3.10)$$

The relationship between the different spectral densities can now be shown as:

$$S_\phi(f) = 2\epsilon(f) = \frac{f_o^2}{f^2} S_Y(f) = \frac{1}{f^2} S_{\Delta f}(f)$$

CHAPTER FOUR
PHASE NOISE MEASUREMENTS

Importance of Phase Measurements

While amplitude noise is the concern of the amplifier designer, phase noise is the concern of the clean oscillator designer since it is the limiting factor in most RF and microwave systems. With the increasing sophistication of these systems, and additional bands being added to the electromagnetic spectrum, modern high-quality signal sources require larger signal power to phase noise power ratio at offset frequencies closer to the carrier, i.e., -80 dB_c per Hz and -160 dB_c per Hz in the range of 20Hz-50KHz.

Two of the phase noise limitations in actual systems can be seen in figures 4 and 5. In Figure 4, the sidebands of a noisy local oscillator in a multichannel communication receiver will also be present at the same ratio in the IF. The sensitivity will then be set by the level of the sidebands, and a weak wanted signal could be buried in the phase noise. In Figure 5, a constellation diagram for an M-ary digital modulation technique shows how phase noise affects the performance of the system. If the reference was smaller or

larger than 45° , due to phase noise, then the probability of incorrectly decoding the signal would increase.

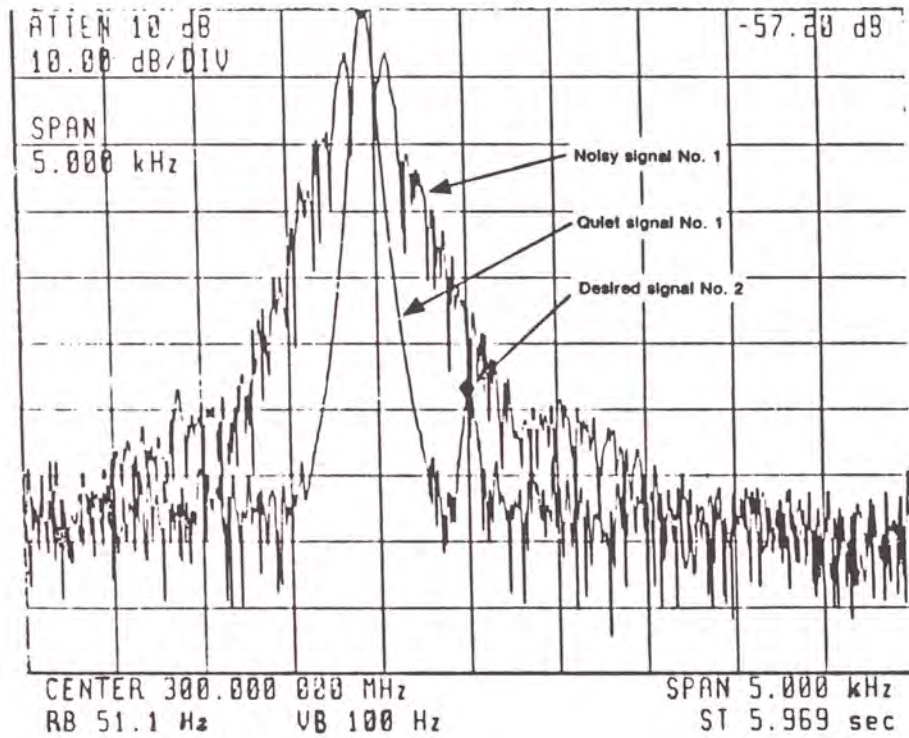


Figure 4. Effect of high level sidebands.
(Moulton 1986)

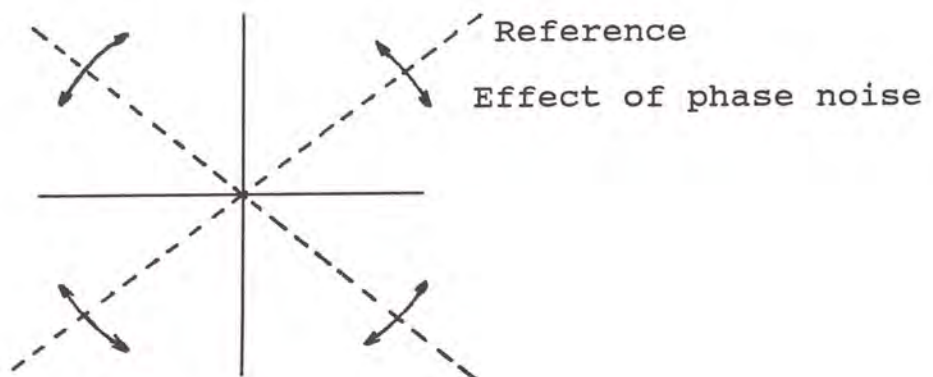


Figure 5. Phase noise effect on a QPSK system.

Random Noise Corrections

Signals derived from real, physical processes are most likely random, or a mixture of deterministic and random such as in the output of a noisy oscillator. Measuring these random processes involves some difficulties not encountered in measuring deterministic signals, and some corrections will have to be made. These measurements depend on some statistical basis, and the process usually consists of taking the rms of an integration or average result. These correction factors do not apply to deterministic signals.

Noise power equivalent bandwidth (B_{Wn}) is an ideal rectangular filter with the same area or power response as the actual IF filter. A simple method to correct for this B_{Wn} which gives accurate results (Hewlett-Packard 1974) is to multiply the IF bandwidth by 1.2.

Once the B_{Wn} is known the next correction factor is for normalization. Because of the randomness of the phase spectrum, doubling the measurement bandwidth doubles the measured power. This requires that random noise be normalized to a per Hz basis. This is easily accomplished with the following relation

$$10 \log \frac{\text{B}_{Wn} \text{ (Hz)}}{1 \text{ (Hz)}} \quad [\text{dB}]$$

Another source of error when making noise measurements occurs in the detector and logarithmic circuitry. Most analyzers use an envelope detector calibrated to read the true rms level of a discrete signal. When this is used with random noise it creates a reading which is lower than the true level. Analyzers have logarithmic IF amplifiers which amplify the noise peaks less than the rest of the noise. Considering that the envelope of random noise is described by the Rayleigh distribution (Reference Data for Radio Engineers 1956), the correction factor required for this circuitry can be found.

Suppose we have a sine wave with a normalized rms value of 1. The analyzer processes this signal by envelope detection, logging, and averaging, that is

$$\overline{V_s} = \ln\sqrt{2} = 0.346$$

Now consider a random noise process with an envelope R described by the normalized ($\sigma = 1$) Rayleigh distribution

$$P(x) = \begin{cases} x \exp \left[-\frac{x^2}{2} \right] & , \quad x > 0 \\ 0 & , \quad \text{otherwise} \end{cases}$$

Following the same procedure as for the sine wave, but using the random processes concept of statistical average

$$\begin{aligned} \overline{V_n} &= \int_{-\infty}^{\infty} V(x) P(x) dx \\ &= \int_0^{\infty} \ln(x) x \exp \left[-\left(\frac{x^2}{2} \right) \right] dx \\ &= 0.058 \end{aligned}$$

A very simple numerical integration program (listing is given in Appendix B) was used to solve the otherwise complicated integral. The difference between the deterministic and random case is 0.288 nepers or 2.5 dB. This value has to be added to the random noise readings to correct for the analyzer circuitry.

Measurement Techniques

Three of the most commonly used methods will be briefly introduced in this section to gain an understanding of the mechanics involved in phase noise measurements. For a more detailed description of these methods see Scherer (1986) and Vendelin(1982).

When the noise sidebands are high enough to be measured directly, the easiest technique would be to view the oscillator spectrum directly on the spectrum analyzer. After applying the random noise corrections at the desired offset frequencies (f_m), and using equation 3.6, the $\mathcal{P}(f_m)$ spectral density can be found.

This method, however, has its limitations since a "clean" oscillator will require measuring sidebands which are beyond the dynamic range of the spectrum analyzer. Another of its limitations would be the reading accuracy at offset frequencies close to the carrier. The next two methods use a carrier suppression technique to solve for those two problems.

In these two techniques it is assumed that the reference source has much lower phase noise than the source.

A Frequency Discriminator is a circuit that yields an output proportional to the frequency deviation of the input. When the oscillator under test and a reference oscillator feed a mixer the random sidebands generate frequency fluctuations, these fluctuations are demodulated and the voltage at the output of the discriminator is the analog of the frequency fluctuations. This technique, then, will give the spectral density of frequency fluctuations, $S_{\Delta f}$.

The Phase Quadrature Detection is a more sensitive method and the most widely used. In this case the oscillators are set at the same frequency and, as before, a mixer and a low pass filter are used as a phase detector. Both inputs to the mixer should be in phase quadrature to ensure maximum phase sensitivity. For ideal oscillators the output at the low pass filter should be 0 volts. The actual voltage, however, is

$$V_o = k \sin (\Delta\theta)$$

for small fluctuations

$$V_o \approx k \Delta\theta$$

and the phase fluctuations can be measured directly. The feedback loop in the system is used to prevent the oscillators from losing phase quadrature. The reference oscillator in the feedback loop is usually a VCO. Figures 6 and 7 show the block diagrams for these two methods.

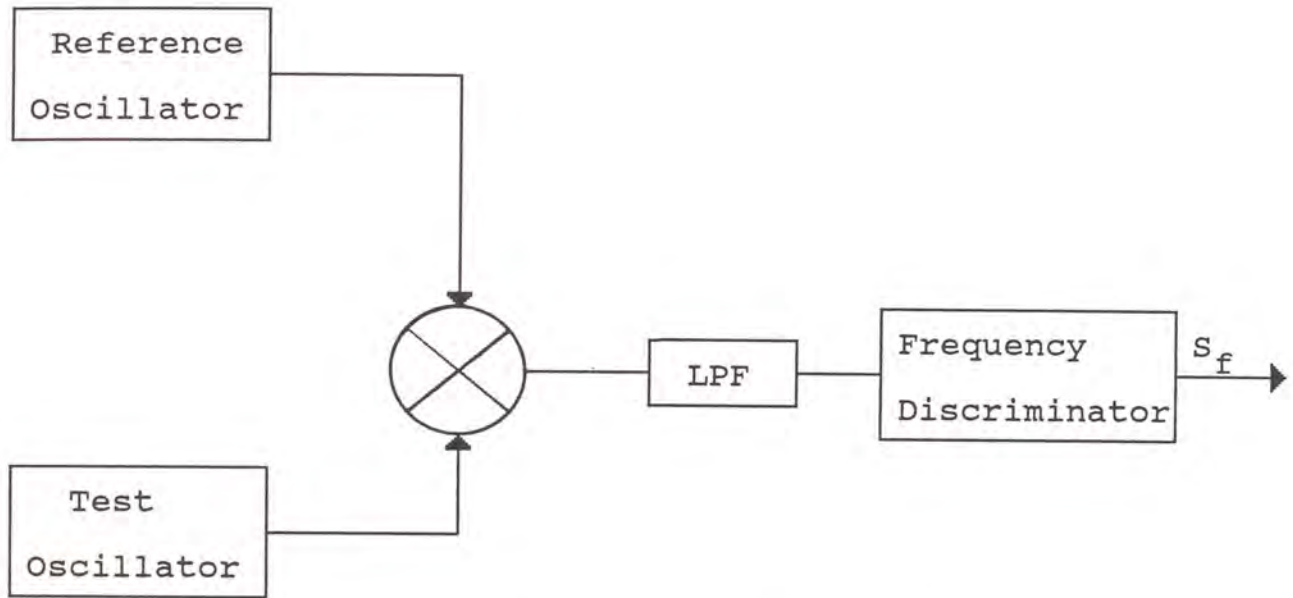


Figure 6. Frequency discriminator system.

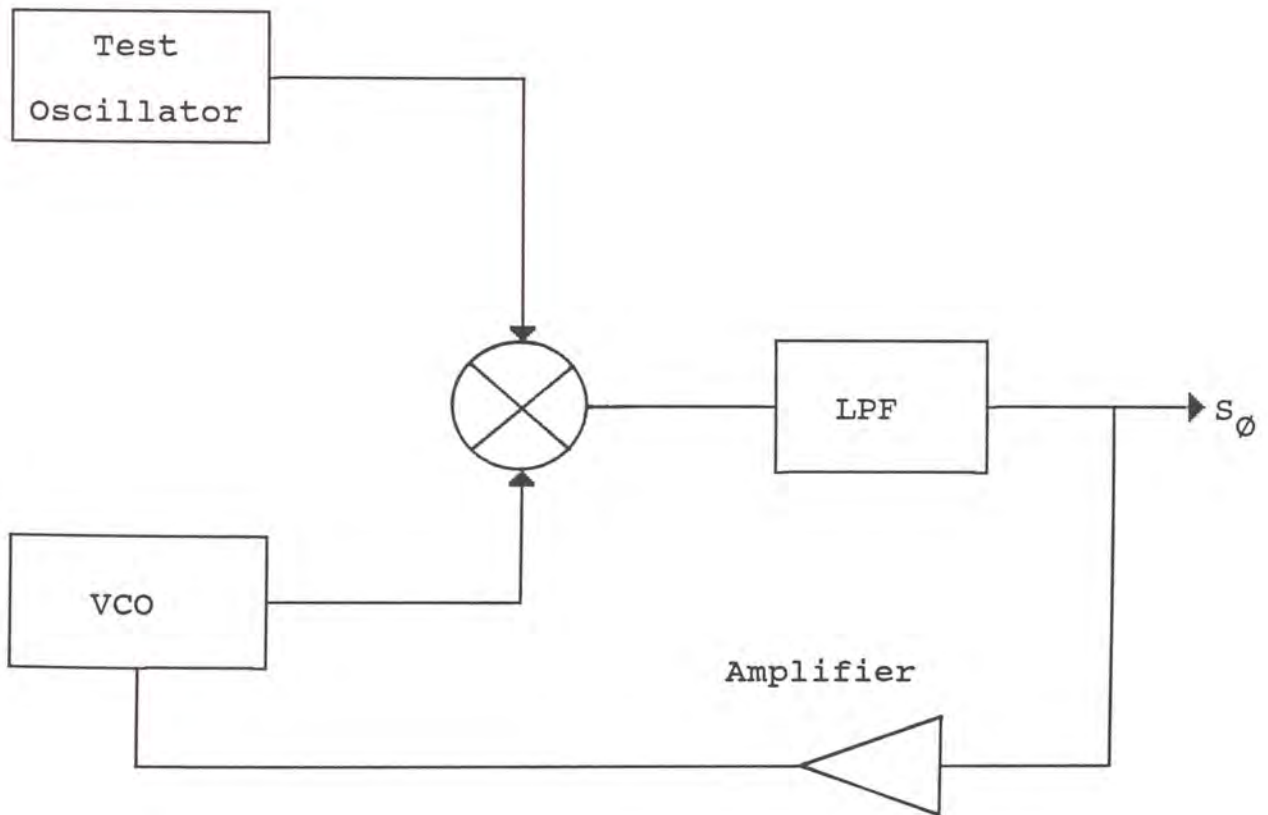


Figure 7. Phase quadrature system.

CHAPTER FIVE

100 MHz OSCILLATOR DESIGN

A source of phase noise, an oscillator, was needed in order to take measurements. A common base Colpitt's oscillator that offers a good performance up to the UHF range (Krauss et al. 1980) was chosen; see Figure 8. In case extra tuning was required, a varactor diode was added for voltage controlled tuning. There are three fundamental parts in an oscillator: an amplifier, a resonator, and an output load. The frequency of operation is determined by the resonator or tank circuit. The Colpitt's resonator consists of an inductor in parallel with a tapped capacitor.

Oscillator Analysis

The oscillator transistor will be modeled by the equivalent circuit of Figure 9. The experimental results obtained with this model show that it is a good approximation for most oscillators (Krauss et al. 1980).

Looking at Figure 8 the circuit elements will be defined: L , C_1 , and C_2 form the Colpitt's resonator or tank

circuit. R_1 , R_B , and R_E establish the DC bias conditions. R_e increases the transistor input impedance, causing its input inductance to be negligible. C_C and C_L are low impedance blocking capacitors. C_B is a bypass capacitor that shorts the base to ground. C_f is a variable capacitor used to tune the frequency. R_L is the load impedance, or input impedance of the measuring device.

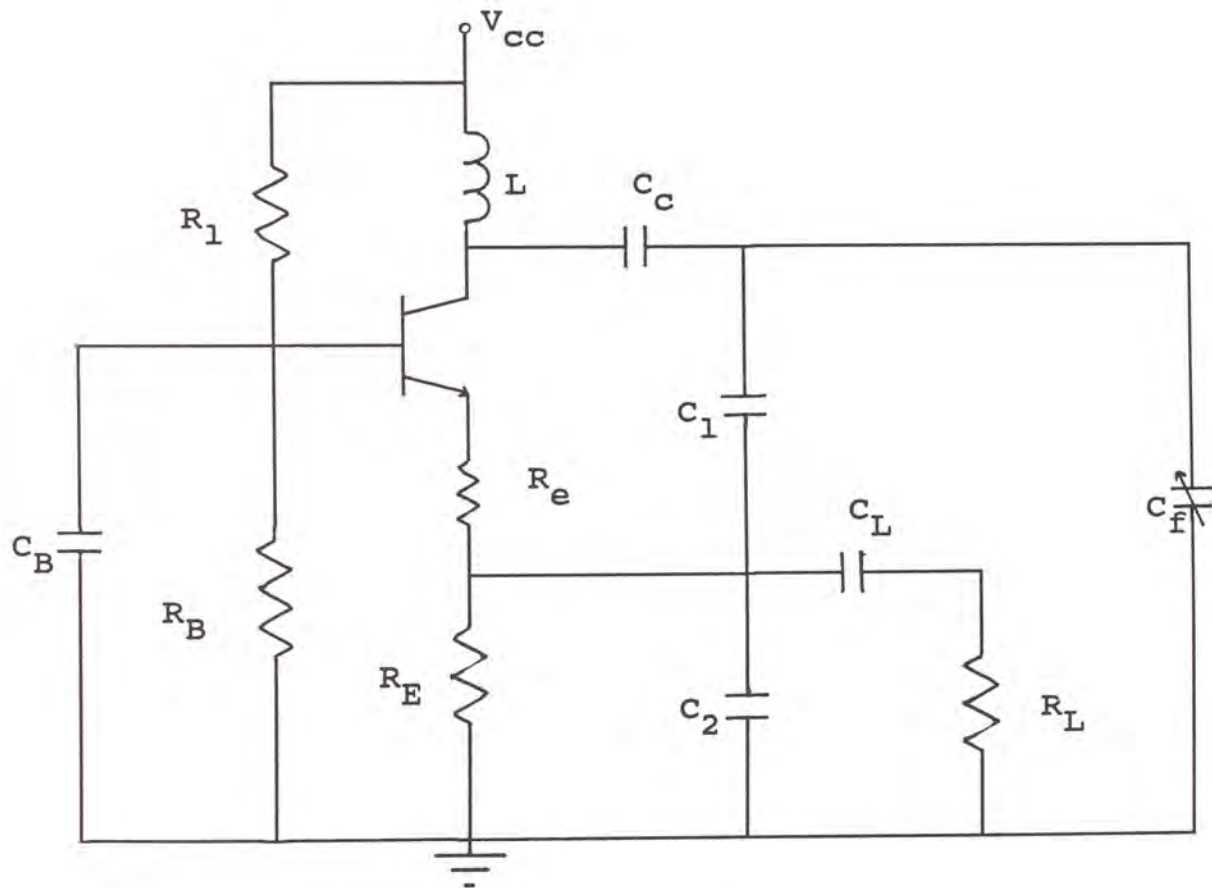


Figure 8. Colpitt's oscillator.

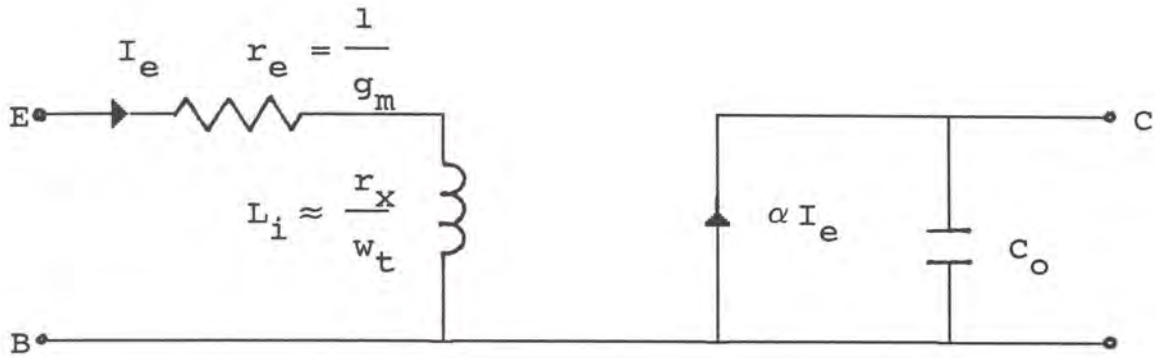


Figure 9. Equivalent transistor model.

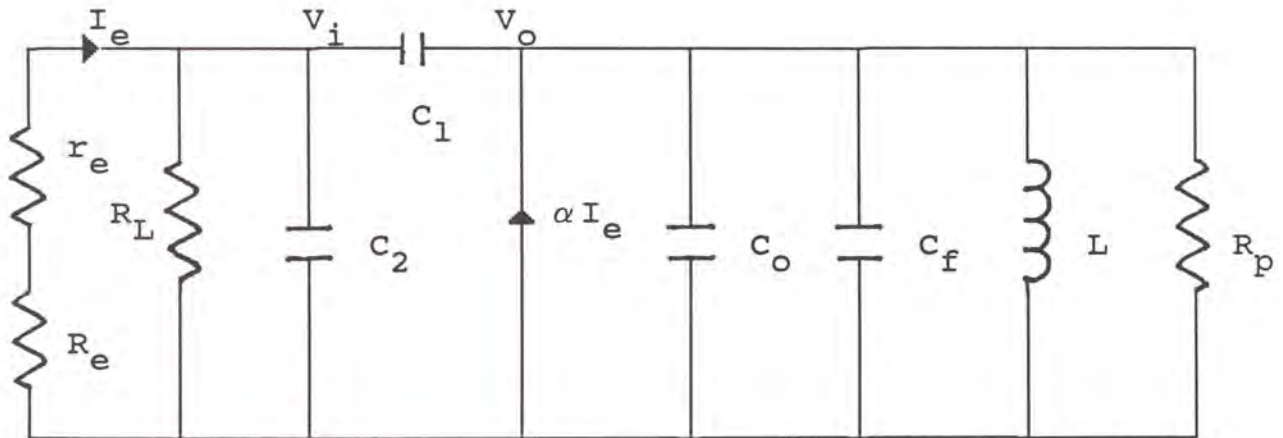


Figure 10. Equivalent oscillator model.

Assuming that the reactances of the bypass and blocking capacitors are zero, the equivalent circuit for the oscillator is shown in Figure 10. $R_i = (R_e + r_e)$, $I_e = -g_i V_i$, and R_p is the equivalent parallel resistance of the inductor.

To facilitate the mathematics, the node equations will be written in terms of admittances. R_2 will be the parallel combination of $(R_e + r_e)$ and R_L .

$$0 = g_i V_i + sC_2 V_i + (V_i - V_o) sC_1$$

$$0 = -g_i V_i + sC_f V_o + \frac{1}{sL} V_o + g_t V_o + V_o sC_1 - V_i sC_1$$

Solving these equations for V_o and assuming an infinitesimal noise pulse input (Krauss et al. 1980), the denominator of V_o will be

$$D = g_2 + s(Lg_p g_2 + C_a) + s^2(Lg_2 C_b + Lg_p C_a - LC_1 g_2) + s^3(LC_a C_b - LC_1^2)$$

where $C_a = C_1 + C_2$, and $C_b = C_1 + C_o + C_f$

Substituting jw for s

$$D = g_2 + w^2 L(C_b g_2 + C_a g_p - C_1 g_2) + j[Lg_p g_2 + C_a - w^2 L(C_a C_b - C_1^2)]$$

For oscillations to occur, this equation must be equal to zero. This condition is met when both the real and the imaginary parts equal zero.

Solving for the imaginary term

$$w_o^2 = \frac{1}{L(C_o + C_f + C_p)} + \frac{1}{R_p R_i (C_1 + C_2) (C_o + C_f + C_p)} \quad (5.1)$$

where $C_p = C_1 || C_2$

Solving for the real term

$$\alpha_{\min} = \frac{1}{1 + \frac{C_2}{C_1}} + \frac{R_i}{R_p} \left(1 + \frac{C_2}{C_1}\right) \quad (5.2)$$

Since $R_p R_i (C_1 + C_2) \gg L$, equation 5.1 can be approximated by

$$\omega_o^2 = \frac{1}{L(C_o + C_f + C_p)} \quad (5.3)$$

This equation shows that the frequency of operation is independent of the transistor parameters; it is determined by the tank circuit.

Equation 5.2 shows a gain restriction. This restriction is not very significant since it will be satisfied if the operating frequency is below one-half f_t , and $R_p > 1000$ ohms (Krauss et al. 1980).

Since the frequency of operation is determined by the tank circuit, the design for L , C_1 , and C_2 will be done with the aid of formulas derived from the tank circuit. These formulas come from the tables in Appendix A. Figure 11 shows the Colpitt's tank circuit.

C_s is defined in the tables as the equivalent series capacitance of C_2 in parallel with R_2 . C is defined as the parallel combination of C_1 and C_s .

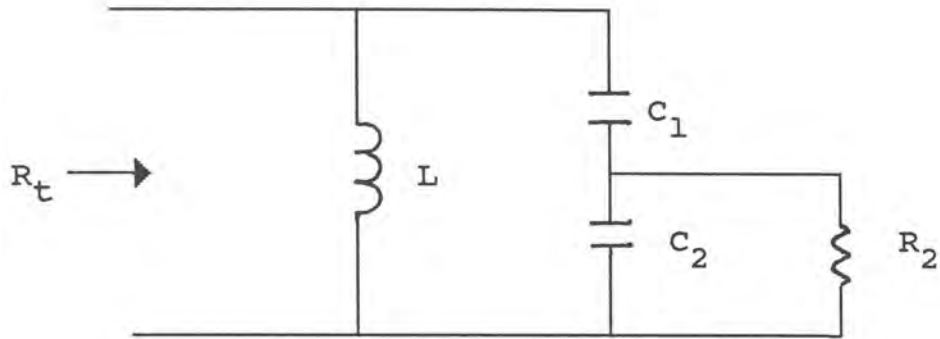


Figure 11. Colpitt's tank circuit.

At resonance the impedance transforming property of the circuit can be modeled by an ideal transformer with turns ratio N . Based on Figure 12

$$\begin{aligned}
 V_i &= NV_o, & V_i I_i &= V_o I_L, & V_o &= I_L R_2 \\
 V_i &= V_o N & & & & \\
 &= I_L R_2 N & & & & \\
 &= N^2 R_2 I_L & & & & \\
 R_t &= N^2 R_2 & & & & (5.4)
 \end{aligned}$$

This turns ratio will be used in the design equations.

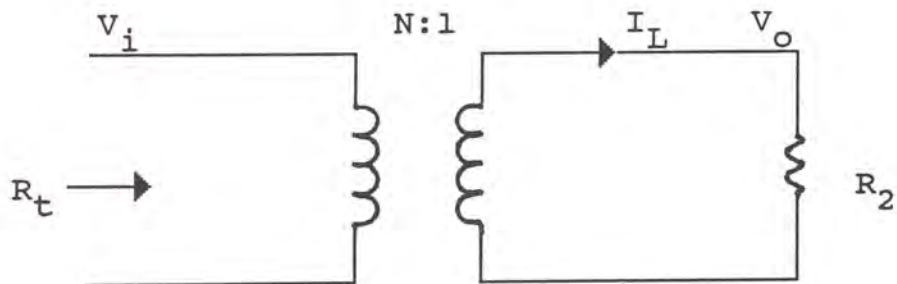


Figure 12. Colpitt's ideal transformer equivalent.

Oscillator Design

The two major considerations in designing an oscillator are the power delivered to the load and the frequency of operation. The input impedance of the spectrum analyzer to be used in the measurements is 50 ohms, the maximum input level at the input mixer is specified not to exceed 13 dBm, and 100 MHz is a frequency in the popular FM band. The oscillator will be designed to operate at 100 MHz, and to deliver 5 mW of power to a 50 ohm load.

In order to design the tank circuit the equivalent parallel resistance of the inductor, the turns ratio N , and the Q of the circuit need to be found. The first step in the design process was to wind an inductor of appropriate size for the frequency of operation and measure its value, and equivalent parallel resistance at 100 MHz. The inductor's impedance measured on the HP 3577A network analyzer was found to be $0.329 \angle 89.57^\circ$. Using the tables in Appendix A, and the program "CL" written for this purpose and listed in Appendix B, the values obtained were

$$L = 26.17 \text{ nH}$$

$$R_p = 2.23 \text{ K}\Omega$$

The inductor value, again referring to the formulas given in the tables of Appendix A, determines the total capacitance needed

$$C_t = \frac{1}{(2\pi f_o)^2 L} = 97 \text{ pF}$$

C_f was selected to be 50 pF, and assuming C_o to be 5 pF

$$C = C_t - C_f - C_o = 47 \text{ pF}$$

Using the result obtained in equation 5.4, the equivalent output circuit of the oscillator is shown in Figure 13.

Letting $R_i = R_L$, and $R_2 = \frac{R_L}{2}$, maximum power is delivered to the load when

$$R_p = N^2 \frac{R_L}{2}$$

which gives

$$N = \left(\frac{2R_p}{R_L} \right)^{\frac{1}{2}} = 9.44$$

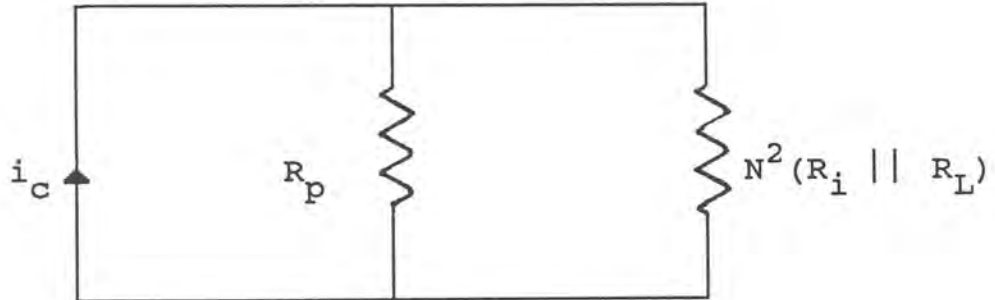


Figure 13. Equivalent output circuit.

The total circuit resistance R_t , is computed to solve for Q_t and Q_p

$$R_t = R_p || N^2 R_2 = \frac{R_p}{2} = 1115 \text{ ohms}$$

$$C_t = \frac{1}{2\pi BR_t}$$

$$Q_s = 2\pi f C_t R_t = 68$$

$$Q_p = \frac{Q_s}{N} = 7.2$$

Using the formulas for $Q_p < 10$

$$C_2 = \frac{Q_p}{\omega_o R_2} = 458 \text{ pF}$$

$$C_s = \frac{C_2 (Q_p^2 + 1)}{Q_p^2} = 467 \text{ pF}$$

$$C_1 = \frac{C_s C}{C_s - C} = 52.2 \text{ pF}$$

The next step is to find the transistor quiescent point so that a biasing network can be designed. The total power delivered by the transistor is given by

$$\begin{aligned} P_T &= \frac{I_C^2 R_t}{2} \\ &= \frac{I_C^2 R_p}{4} \end{aligned}$$

From Figure 13, half of this power goes through R_p and one fourth goes through R_i and R_L , that is

$$P_L = \frac{1}{4} \frac{I_C^2 R_p}{4}$$

$$I_C = 4 \left(\frac{P_L}{R_p} \right)^{\frac{1}{2}} = 6 \text{ mA}$$

I_C sets the value of r_e

$$r_e = \frac{1}{40I_C} = 4 \text{ ohms}$$

since R_i must equal R_L , R_e will be selected to be 47 ohms.

The DC power drawn by the transistor is

$$P_{DC} = V_{CB}I_C = I_C^2 R_t$$

$$V_{CB} = \frac{I_C R_p}{2} = 6.67 \text{ volts}$$

The oscillator's DC circuit is shown in Figure 14.

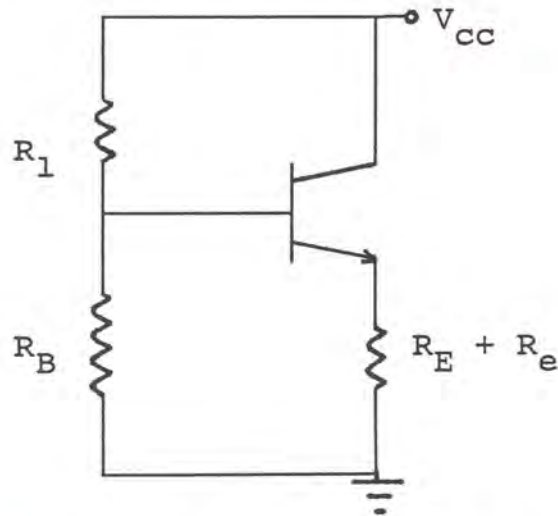


Figure 14. Oscillator's DC circuit.

Assuming $V_{BE} = 0.7$ volts, a DC current gain of 50, a current of 1.5 mA through R_B , selecting R_E to be 620Ω , and this set of equations

$$V_{CC} = V_{CB} + V_{BE} + I_C(R_e + R_E)$$

$$V_B = V_{BE} + I_C(R_e + R_E)$$

$$\frac{V_{CC} - V_B}{R_1} = I_B + \frac{V_B}{R_B}$$

the following values were calculated

$$V_{CC} = 11.4 \text{ volts}$$

$$R_1 = 4.14 \text{ K}\Omega$$

$$R_B = 3.13 \text{ K}\Omega$$

This completes the design. Figure 15 shows the final circuit configuration. The blocking and bypass capacitors were selected to be $0.1 \mu\text{F}$. Small capacitors, 100 pF , were added in parallel across these capacitors to eliminate possible high frequency oscillations.

Results

The designed circuit oscillated at a frequency of 97 MHz with a peak voltage of 0.48 volts which corresponds to 2.3 mW of power. C_f was then varied until the design frequency of 100 MHz was achieved. The smaller power delivered to the load could be due to some RF dissipation through R_E ; this could be avoided by inserting an RF choke in series with R_E . The final oscillating signal used in this paper is shown in Figure 16, which depicts the time domain output, and Figure 17, which depicts the frequency domain output.

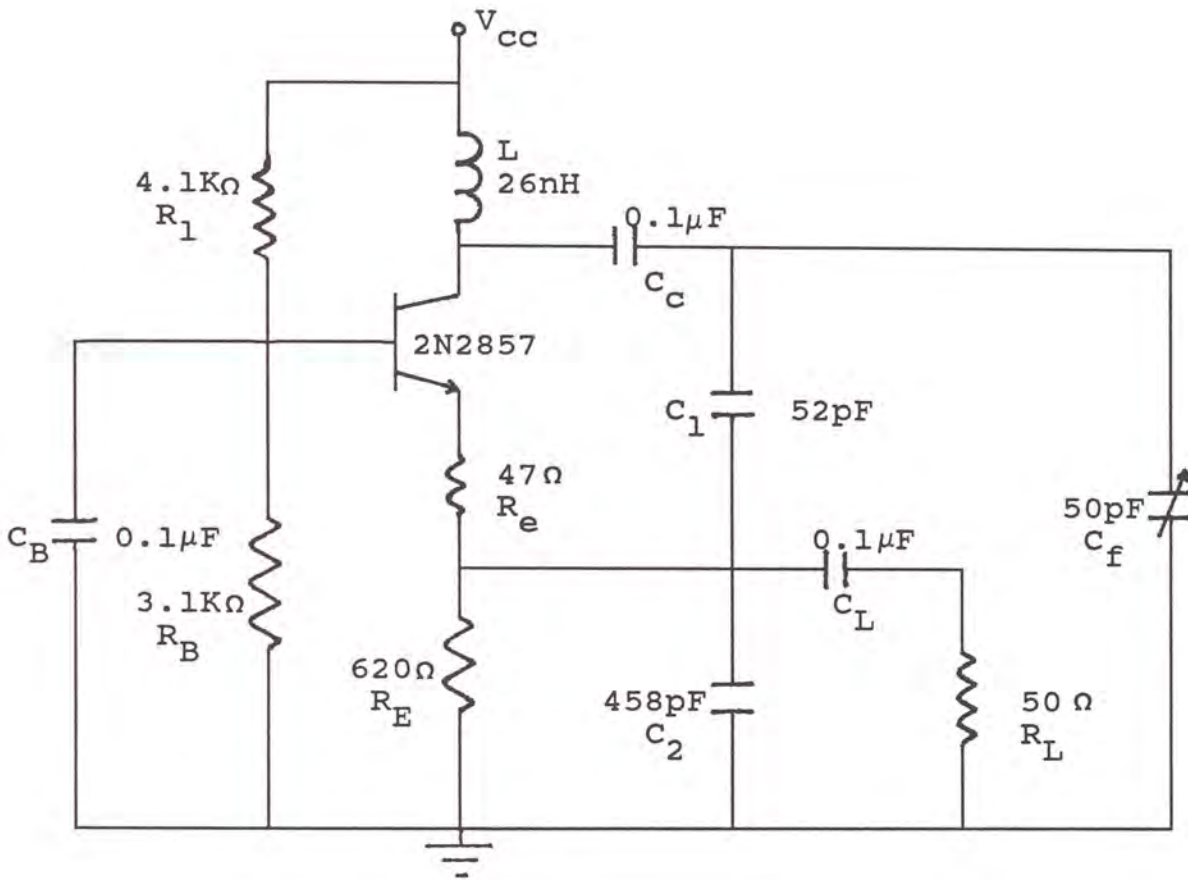


Figure 15. Colpitt's final circuit configuration.

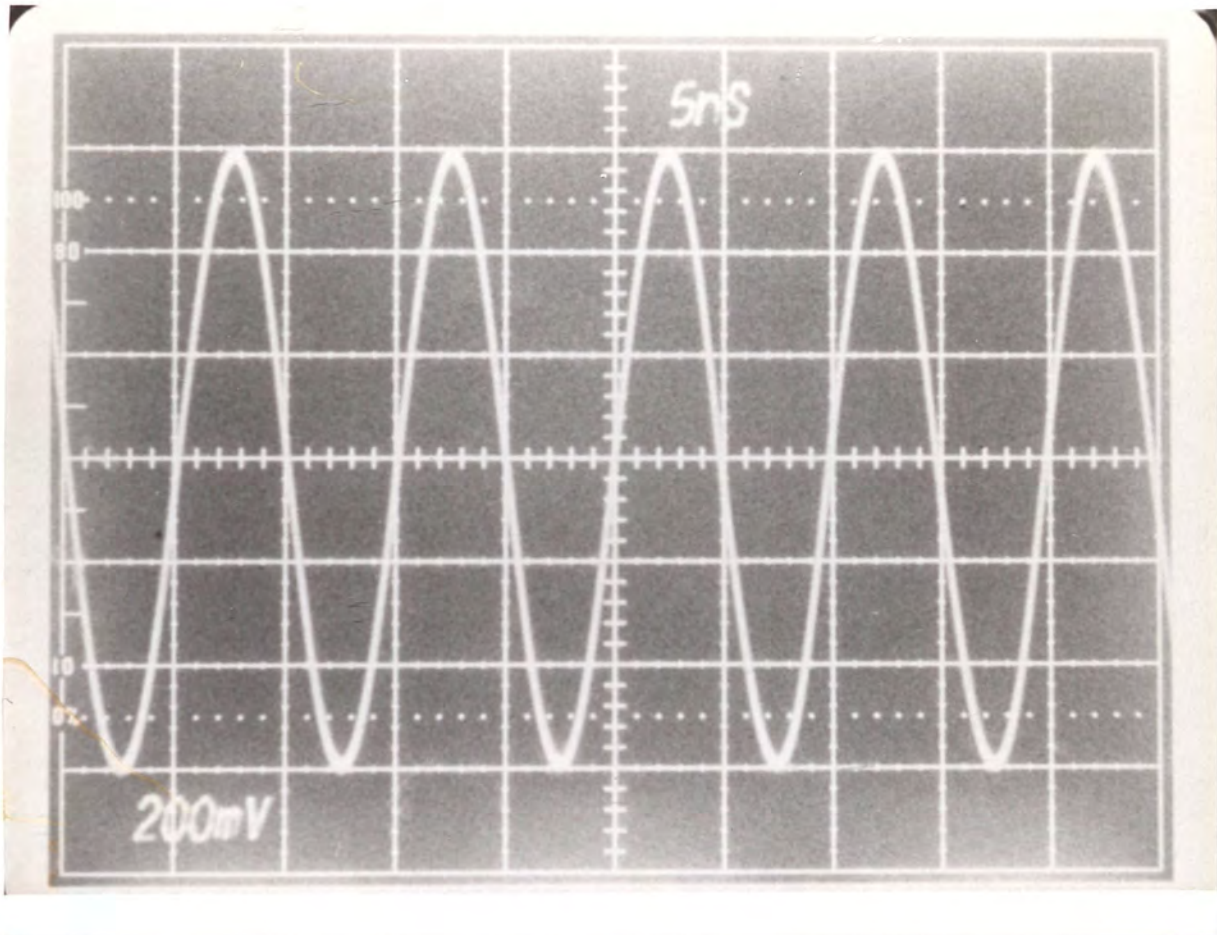


Figure 16. Time domain output.

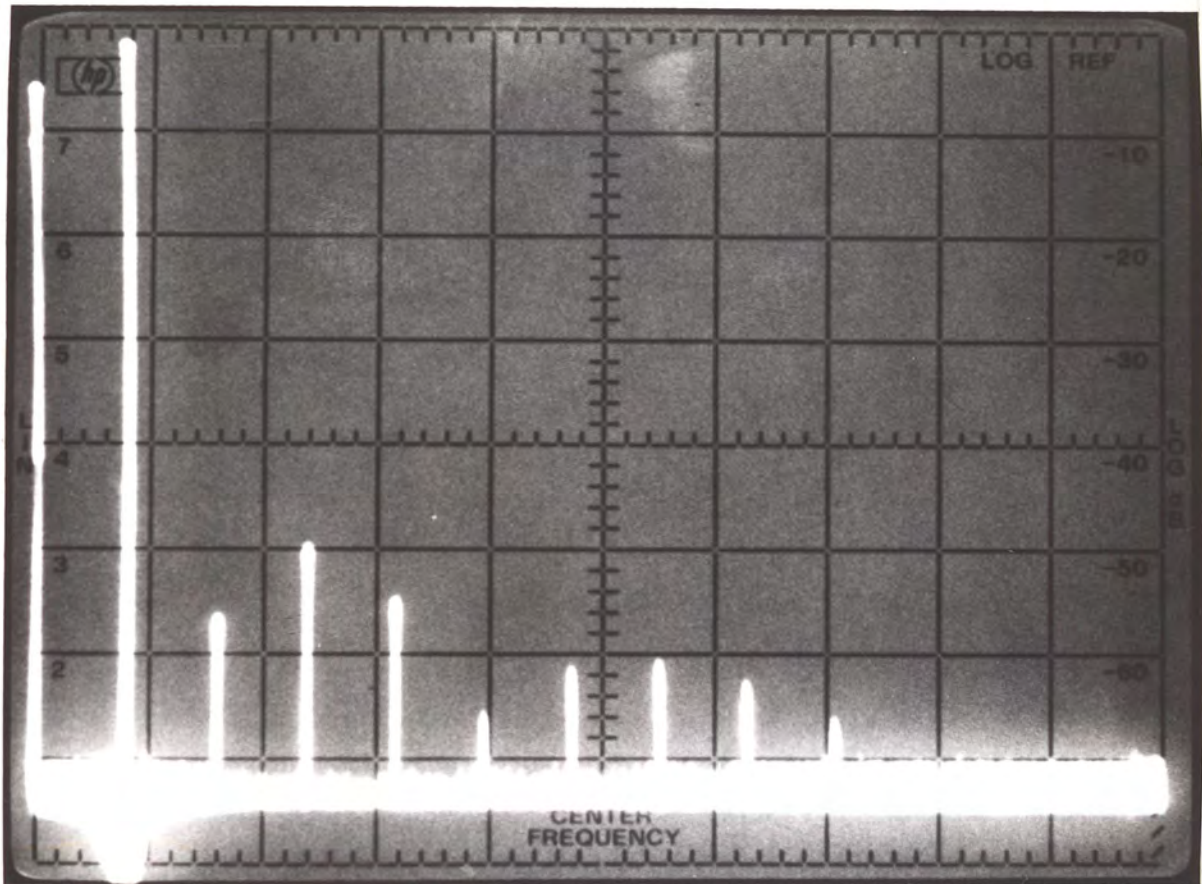


Figure 17. Frequency domain output.

Marker = 100 MHz Scan Width = 0 - 1250 MHz
Vertical = 10 dB/division Reference Level = 3 dBm

CHAPTER SIX
PLL MEASUREMENT TECHNIQUE
DESIGN AND IMPLEMENTATION

System Design

Once the oscillator was designed and tested, noise measurements could then be made. A new technique using a phase-locked loop for phase noise measurement is introduced. This technique uses the same approach as the frequency discriminator but utilizes a PLL instead to accomplish the demodulation. A block diagram of the system is shown in Figure 18.

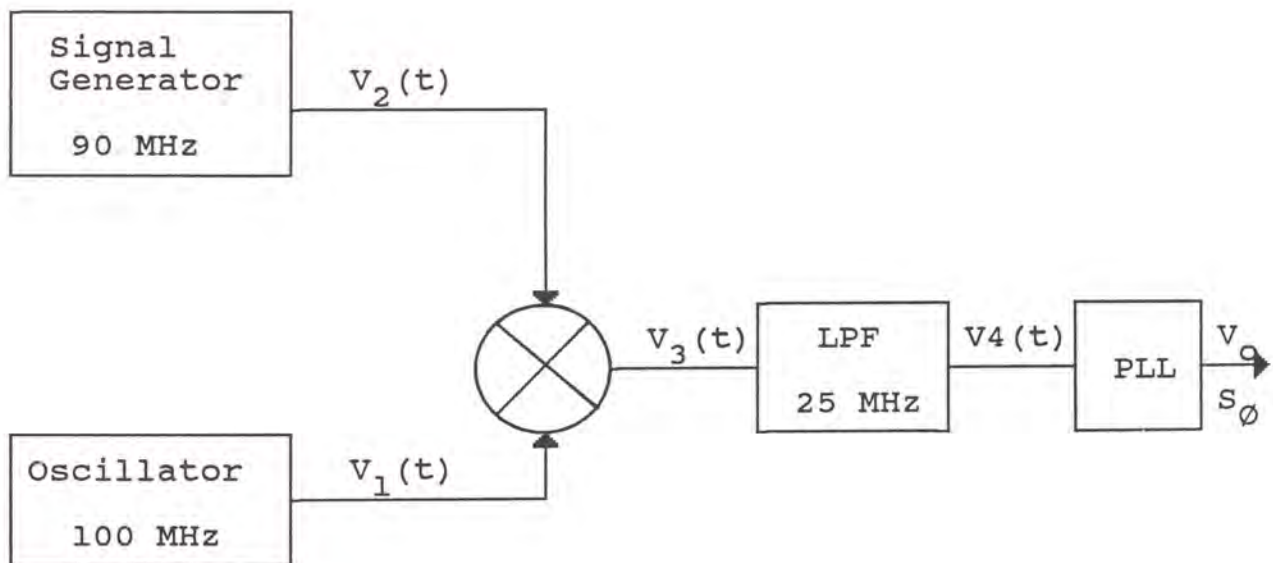


Figure 18. Phase noise measurement system.

A phase-locked loop in integrated form, the XR-215, that operates up to 35 MHz was used. The oscillator output was mixed down with a stable 90 MHz local oscillator, such that the IF frequency is well within the PLL operating range. The sum frequency was filtered out by the low-pass filter, and the phase-locked loop was designed to demodulate at the difference frequency.

The 90 MHz signal was provided by the Hewlett-Packard's Signal Generator model 8654B.

The double balance mixer was an Anzac MD-140.

The low-pass filter design was a third-order Butterworth with a cut-off frequency of 25 MHz.

From a normalized Butterworth table the schematic shown in Figure 19 was obtained

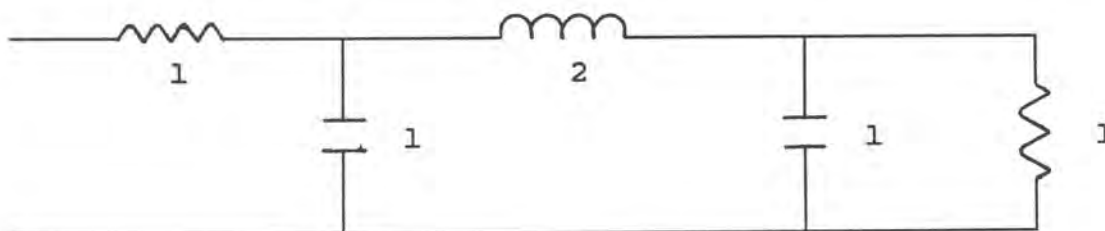


Figure 19. Normalized third order Butterworth

Scaling the elements to $R = 50\Omega$, and $\omega = 2\pi 25 \times 10^6$ radians.

$$L = \frac{2R}{\omega} = 0.6 \mu\text{H}$$

$$C = \frac{1}{\omega R} = 127 \text{ pF}$$

REF LEVEL /DIV OFFSET 26 749 998.662Hz
0.000dB 5.000dB MAG (S21) -3.039dB

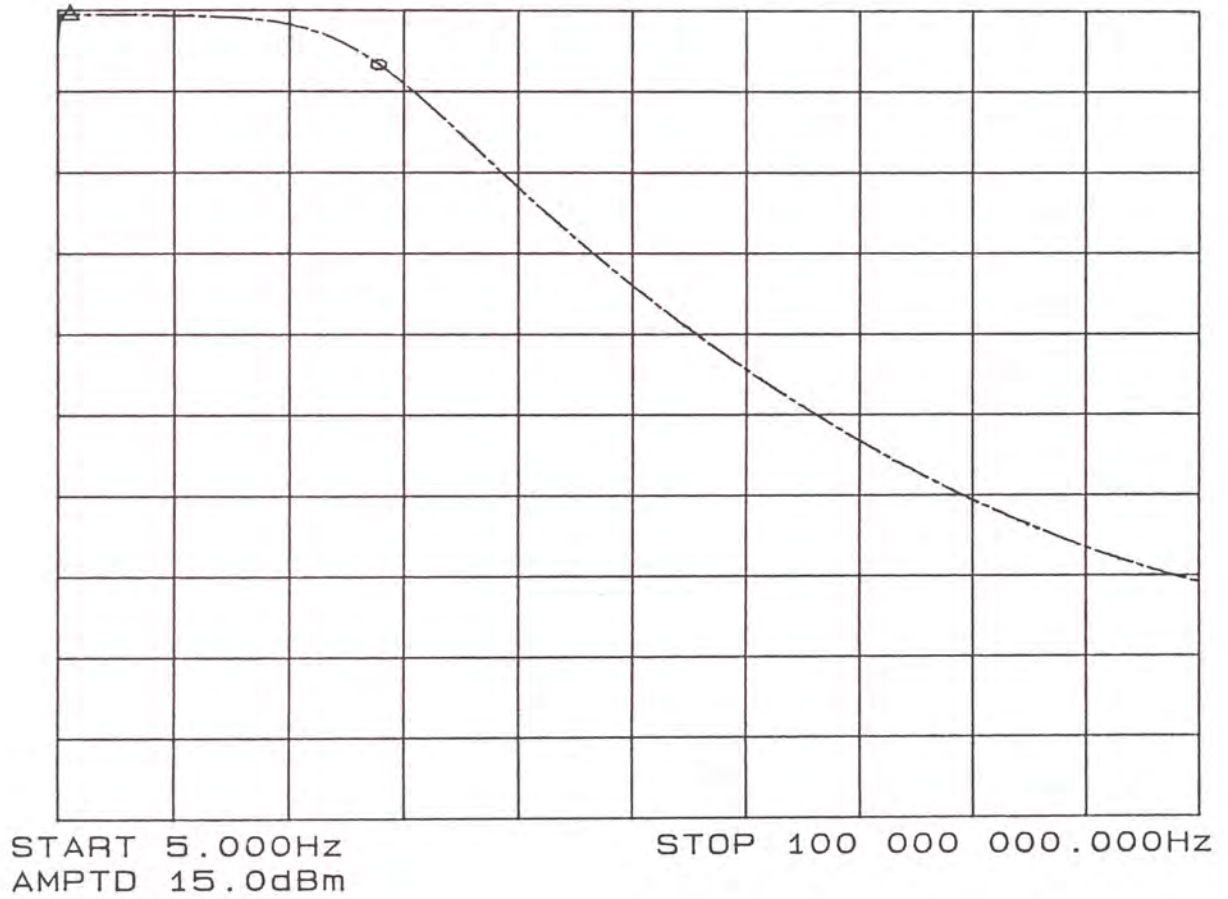


Figure 20. LPF magnitude response.

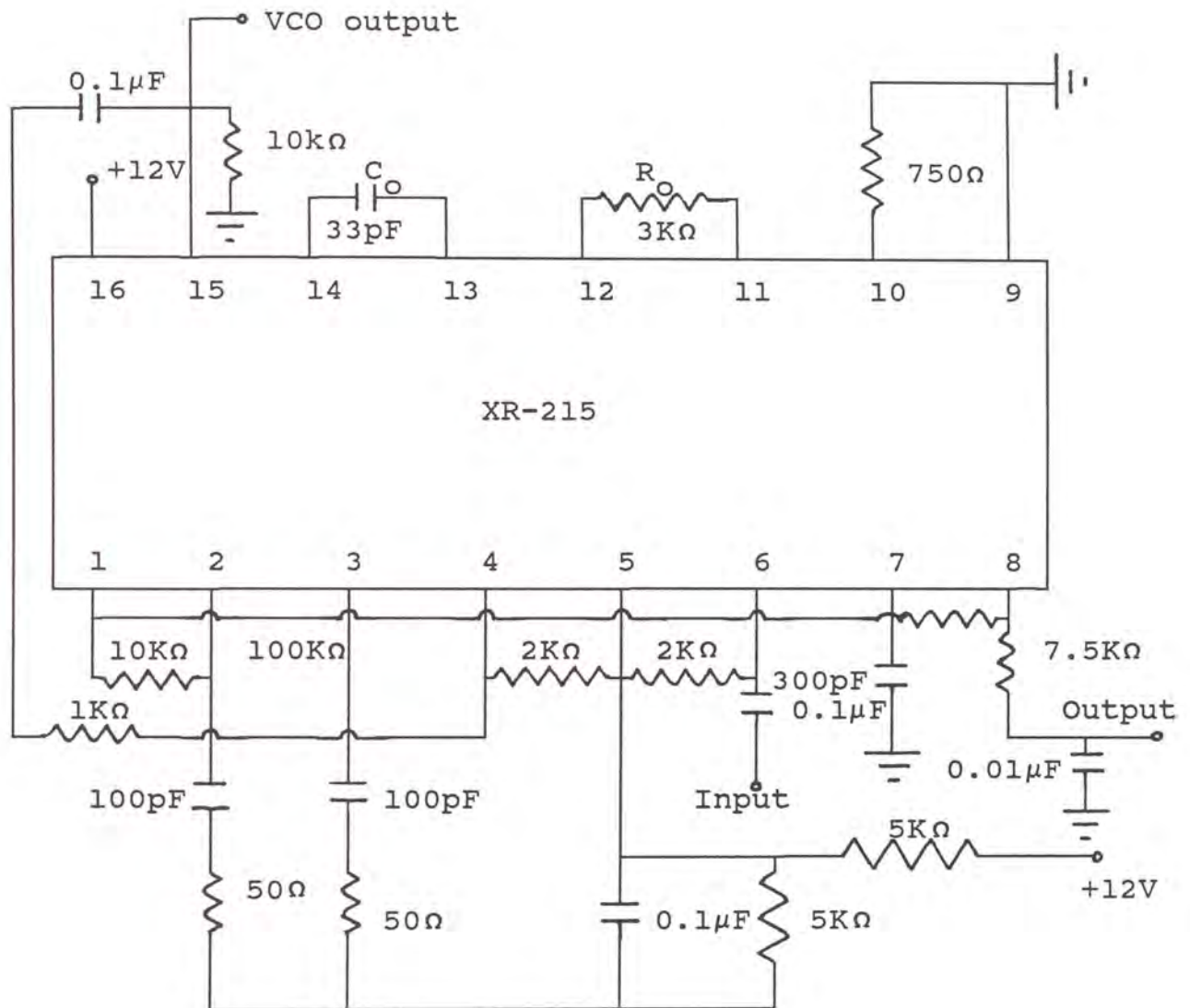


Figure 21. PLL circuit schematic.

The magnitude response of the filter is shown in Figure 20.

The PLL design is shown in Figure 21. The phase comparator inputs are pins 4 and 6. Pin 6 was used as the signal input, and pin 4 was AC coupled to the VCO output. The DC bias for the phase comparator is set at one half V_{cc} at pin 5.

Pins 2 and 3 are the outputs of the phase comparator. The low-pass filter is achieved by connecting an RC network at these two pins.

The VCO free-running frequency is given by (Exar 1979)

$$f_o = \frac{1}{R_o C_o} \quad [\text{Hz}]$$

where R_o is the timing resistor between pins 11 and 12, and C_o is the capacitor between pins 13 and 14. For a free-running frequency of 10 MHz R_o was chosen to be 3 K and C_o was 33 pF.

The resistor between pins 1 and 8 controls the output amplitude. The capacitor at pin 7 is a compensation capacitor for the internal operational amplifier. The resistor at pin 10 is suggested for operation above 5 MHz.

Mathematical Analysis

The output of the oscillator and the local oscillator are given respectively by

$$V_1(t) = A_1 \cos (w_1 t + \phi_1(t))$$

$$V_2(t) = A_2 \cos (w_2 t + \phi_2(t))$$

and

$$f_1 = 100 \text{ MHz}$$

$$f_2 = 90 \text{ MHz}$$

$$f_c = 10 \text{ MHz}$$

$$f_s = 190 \text{ MHz}$$

$\phi_1(t)$ is the oscillator phase noise

$\phi_2(t)$ is the local oscillator phase noise

The mixer output is then given by

$$V_3(t) = A_1 A_2 [\cos (w_1 t + \phi_1(t)) \cos (w_2 t + \phi_2(t))]$$

$$V_3(t) = k_1 [\cos(w_s t + \phi_1(t) + \phi_2(t))] + k_1 [\cos(w_{ct} + \phi_1(t) - \phi_2(t))]$$

where

$$k_1 = \frac{A_1 A_2}{2}$$

the low pass filter output is given by

$$V_4(t) = k_1 [\cos(w_c t + \phi_1(t) - \phi_2(t))]$$

Figure 22 and Figure 23 show that the phase noise of the signal generator is much smaller than that of the oscillator, that is, the overall contribution to the noise comes from the oscillator alone. Had both sources been equally noisy, the phase noise would have been 3dB less than

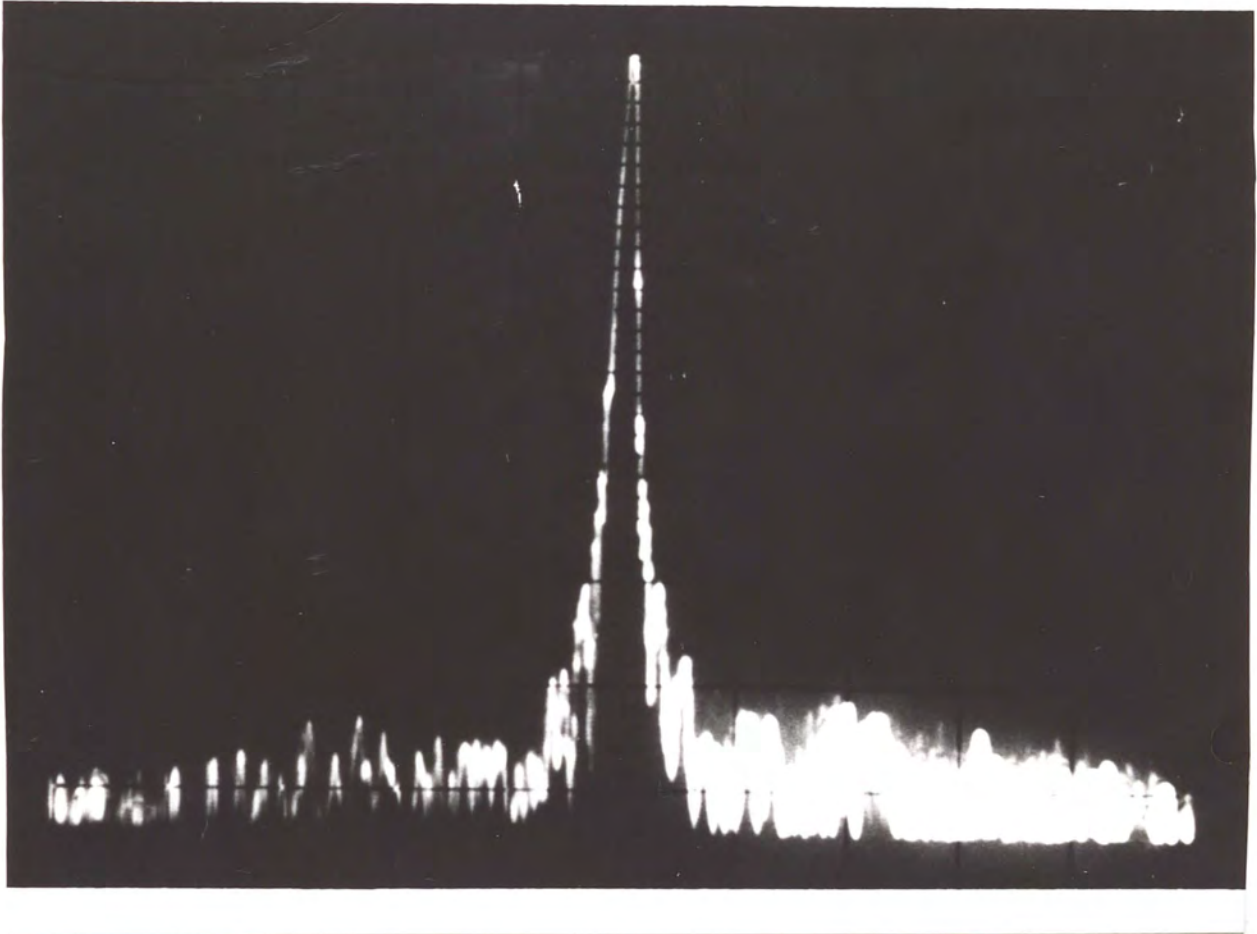


Figure 22. Local oscillator spectrum.

Vertical center line = 100 MHz
Scan Width = 2 KHz/ division

BW = 300 Hz
Vertical = 10 dB/division

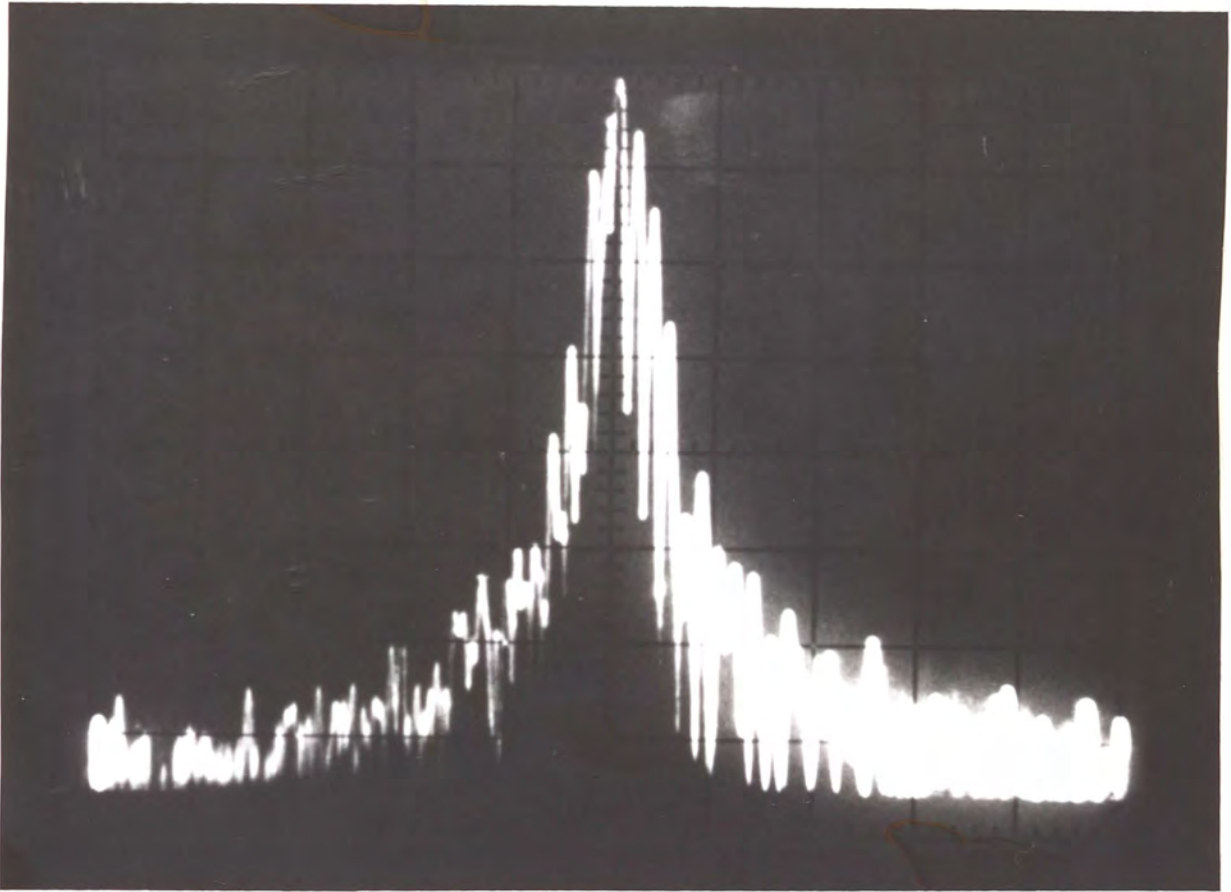


Figure 23. Oscillator spectrum.

Vertical center line = 100 MHz
Scan Width = 2 KHz/ division

BW = 300 Hz
Vertical = 10 dB/division

the measured value. Then, the low pass filter output is given by

$$V_4(t) = k_1 [\cos(\omega_c t + \phi_1(t))] \quad (6.1)$$

The PLL output is proportional to the derivative of the modulating signal (Ziemer & Tranter 1985), that is

$$V_o(t) = K \dot{\phi}_1(t)$$

Squaring both sides, applying the differentiation property of the Fourier transform, and taking into account that the output voltage was read by the spectrum analyzer in

$$\frac{\text{dBV}}{\sqrt{\text{Hz}}}, \text{ that is } \frac{V_{\text{rms}}}{\sqrt{\text{Hz}}}$$

$$(V_{\text{rms}})^2 = K^2 (2\pi f_m)^2 S_{\phi}(f_m)$$

$$S_{\phi}(f_m) = \frac{(V_{\text{rms}})^2}{4\pi^2 K^2 f_m^2} \quad (6.2)$$

Calibration

Equation 6.2 shows that the spectral density of phase fluctuations can be read directly at the output of the PLL. Before this can be done one more step needs to be taken, that of calibrating the system to find the constant K.

For sinusoidal modulation, substituting the modulating signal for $\phi_1(t)$ in equation 6.1

$$V_4(t) = k_1 \cos(\omega_c t + \beta \sin \omega_m t) \quad (6.3)$$

$$V_o(t) = K\beta w_m \cos w_m t$$

$$V_o(t) = K \left[\frac{\Delta f}{f_m} 2\pi f_m \right] \cos w_m t$$

$$V_o(t) = K [2\pi\Delta f] \cos w_m t \quad (6.4)$$

$$K = \frac{V_{op}}{2\pi\Delta f} \quad (6.5)$$

where Δf is the peak frequency deviation.

Figure 24 shows the system designed to measure K.

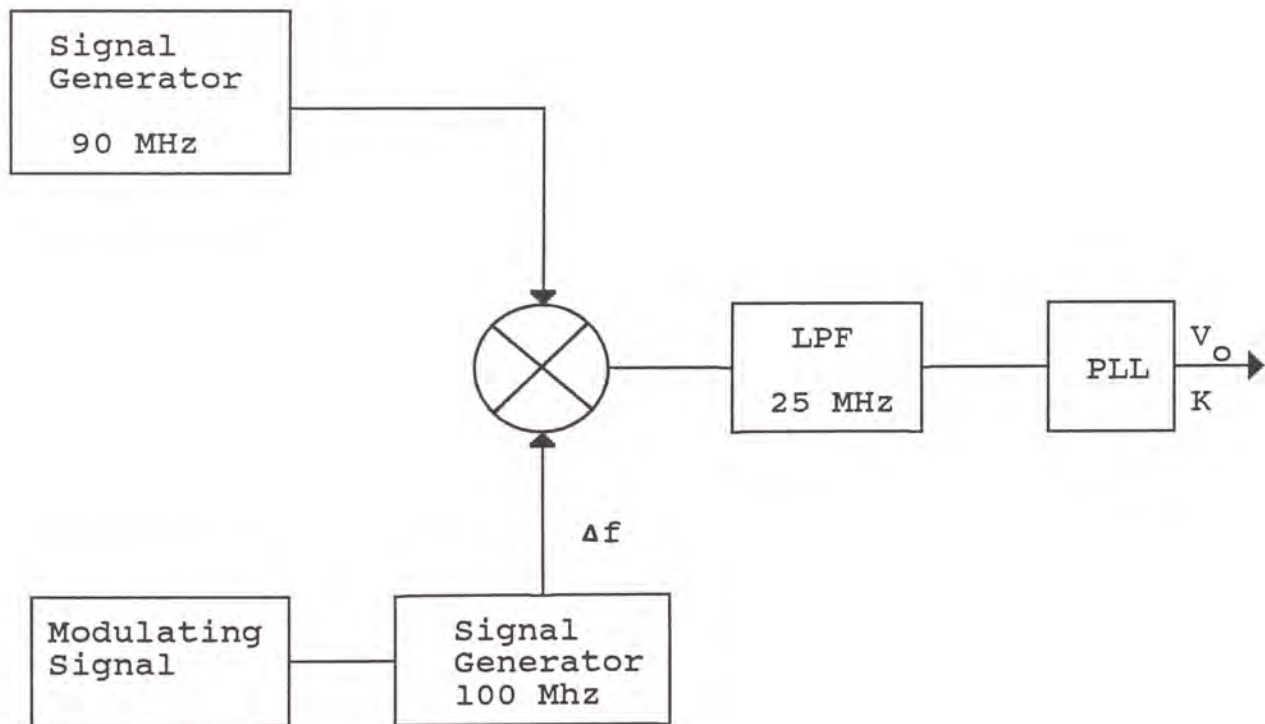


Figure 24. Calibration system.

The oscillator was replaced by a signal generator which was externally FM modulated by a sinusoidal input. The effect of this modulation was shown in equations 6.3 and 6.4.

Varying the input voltage of the modulating signal, different frequency deviations were obtained. By reading these frequency deviations directly from the signal generator, and recording the demodulated output voltage, the constant K was found using equation 6.5. The results of the calibration are shown below:

Vo (mVp)	Δf (KHz)	$K \left(\frac{V_p}{\text{rad}} \right)$
22	2.78	$1.26 \cdot 10^{-6}$
70	8.80	$1.26 \cdot 10^{-6}$
220	27.8	$1.26 \cdot 10^{-6}$

K was measured as volts peak, but realizing that the correct unit of equation 6.2 is H^{-1} , the constant will have to be modified

$$K = \frac{1.26 \cdot 10^{-6}}{\sqrt{2}} = 8.91 \cdot 10^{-6} \frac{V_{rms}}{\text{rad}}$$

Measurements and Results

The first phase noise measurement taken was that of the $f(fm)$ spectral density. This measurement was taken so that further measurements could be compared to prove their validity. The measurements were taken by connecting the oscillator output to the spectrum analyzer (HP 8554B) and following the procedure given in chapter 4. Figure 23 shows a picture of the oscillator spectrum taken at a bandwidth of 300 Hz and a scan width of 2KHz per division from which the measurements were taken. The result is shown in Figure 25.

S_{ϕ} was measured using the set up of Figure 18. A low frequency spectrum analyzer was used for this measurement (HP 3582A). The corrections for BWN and normalization were not needed in this case because, as mentioned before, this advanced analyzer takes into account the BWN and normalization factors giving the readings directly in dBV per square hertz. Figure 26 is a picture of the spectrum of the demodulated phase noise. The dBV were converted to V_{rms} , and then used in 6.2 to obtain S_{ϕ} . Following the relation

$$f(fm) = \frac{1}{2} S_{\phi}$$

3 dBs were subtracted from the readings so that $f(fm)$ could be plotted. A program listing of this process is given in Appendix B. The result is shown in Figure 27.

Comparing the results of both measurements, figures 25 and 27, it can be seen that they are very close up to about 5 KHz. At this point the curves start diverging, and at an offset of 25 KHz the difference is 20 dB. This difference can be explained in terms of the limitations of the HP 8554B spectrum analyzer which has a maximum dynamic range of 70 dB. Also, the system noise floor seems to be a limiting factor in the results. By suppressing the carrier with the PLL measurement technique the measurement range was improved at the higher offset frequencies, but not much improvement was achieved at frequencies close to the carrier or DC.

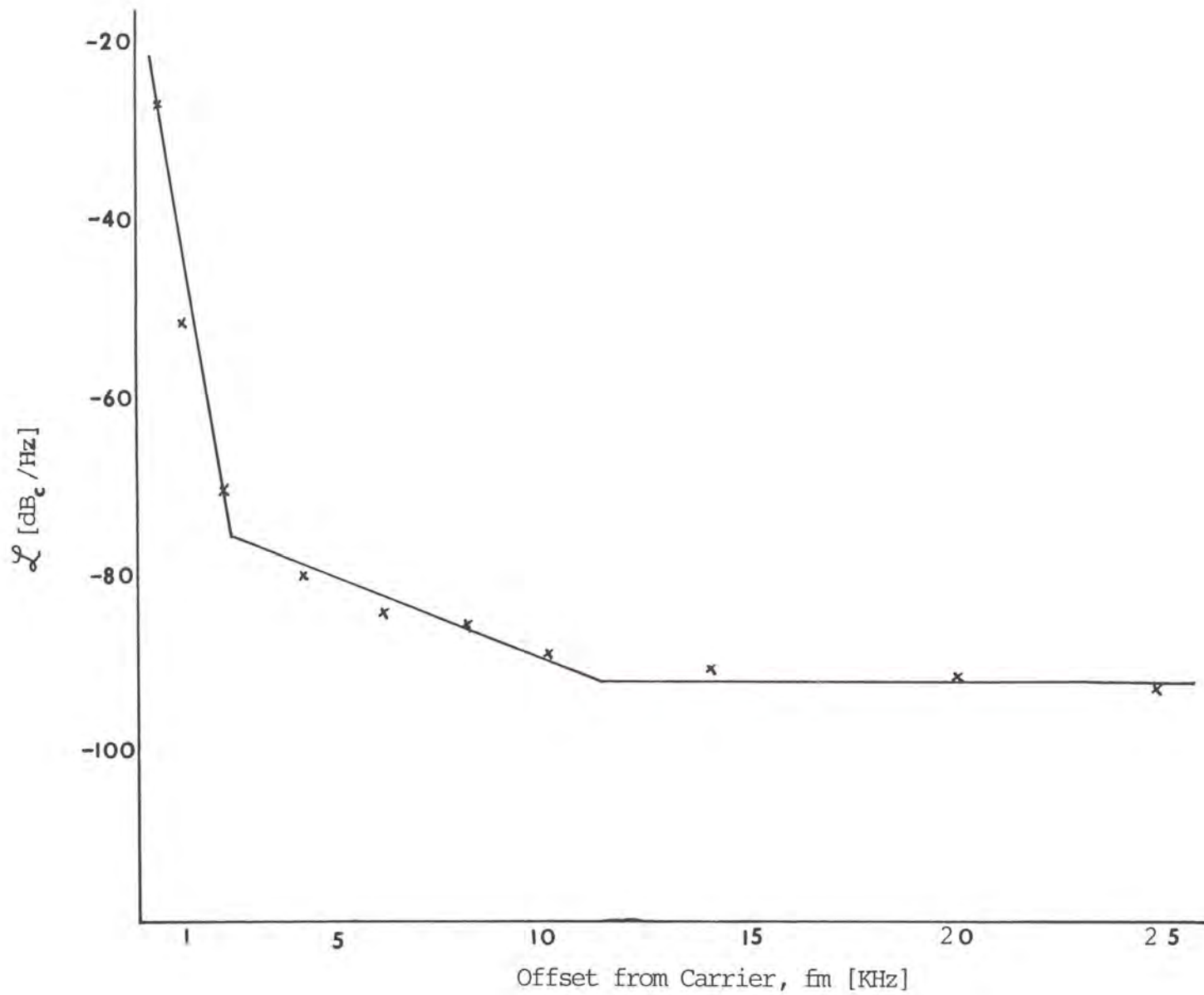


Figure 25. RF phase noise spectrum result.

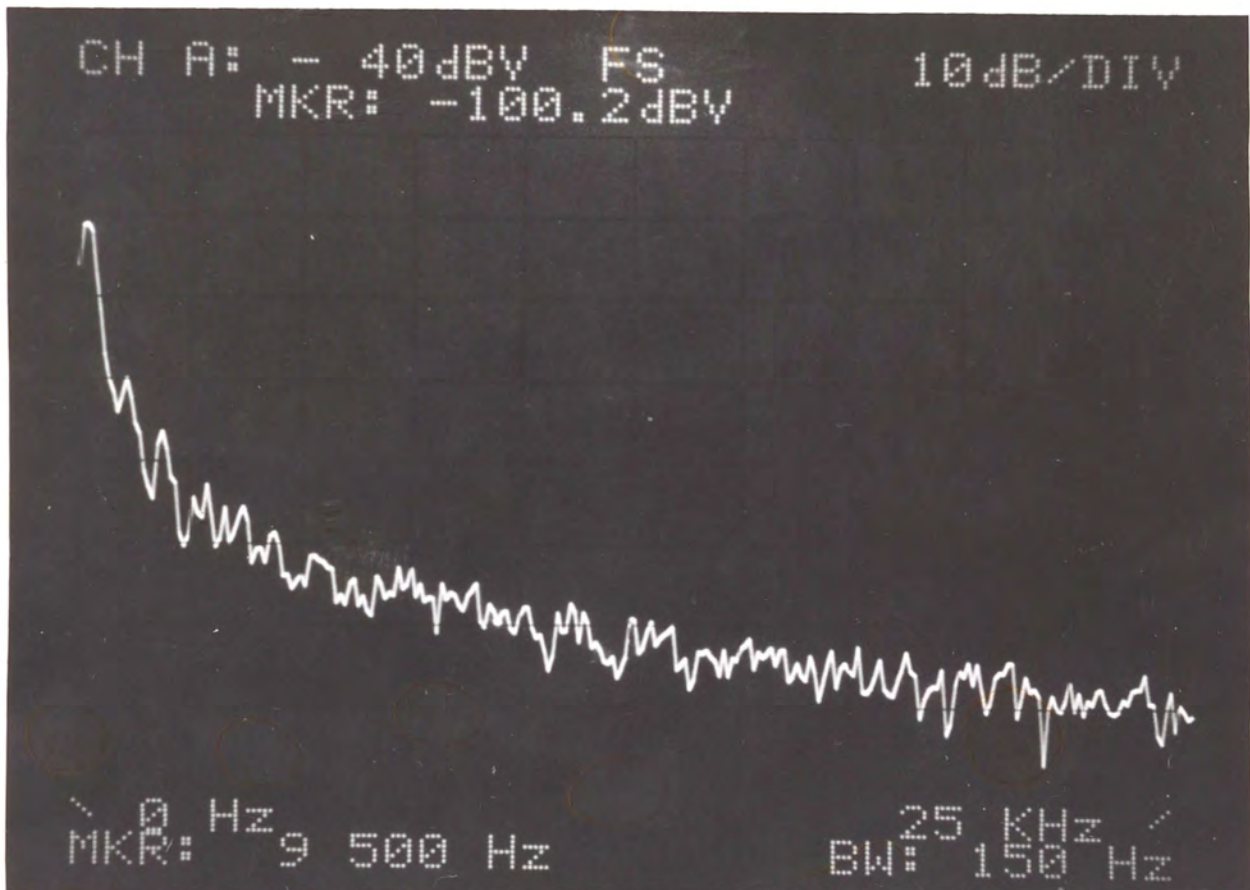


Figure 26. Baseband spectrum of demodulated output.

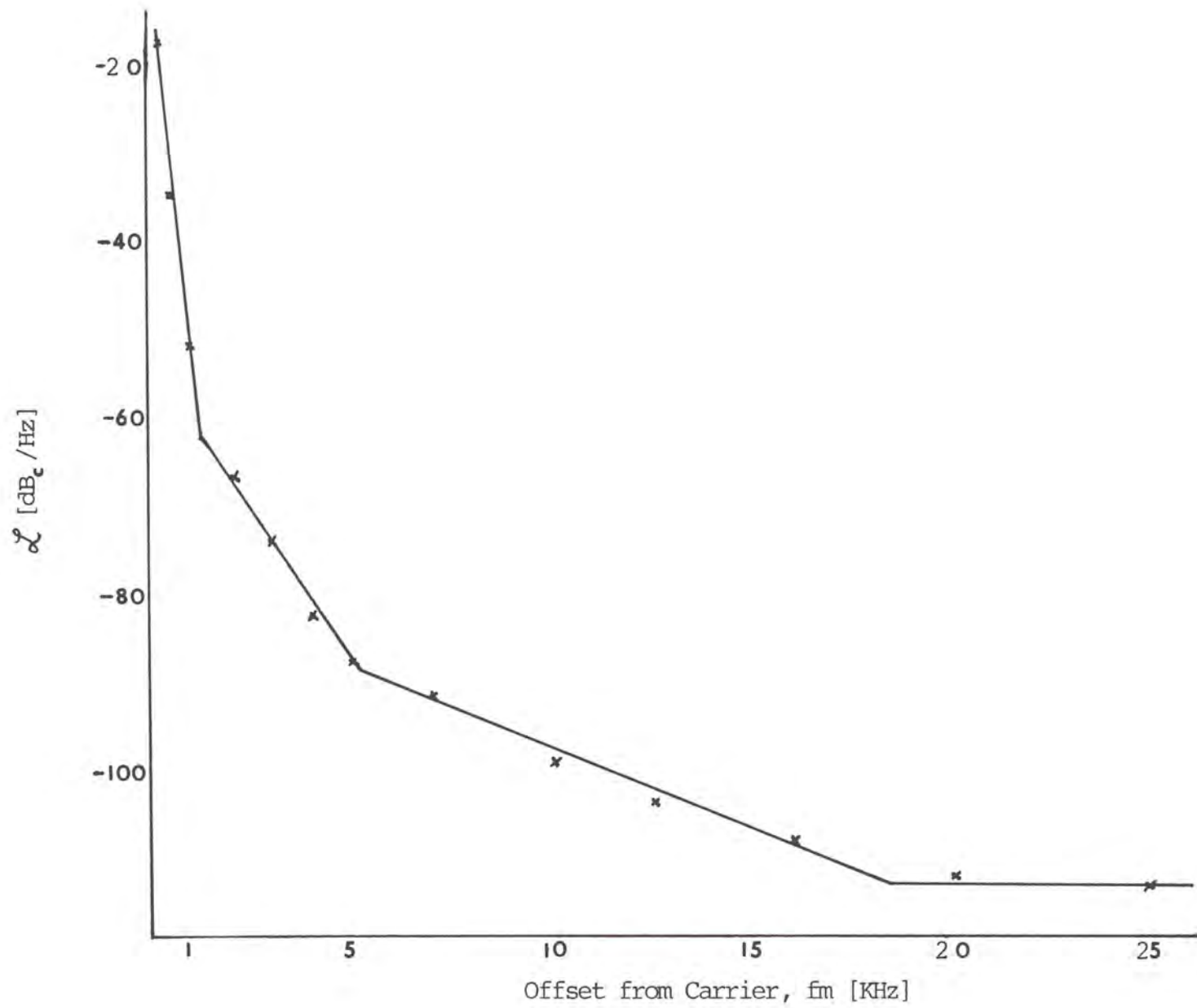


Figure 27. PLL measurement result.

CHAPTER SEVEN

A FEEDBACK MODEL FOR OSCILLATOR PHASE NOISE

Phase noise produces a particular shape or slope on the spectral density graph. Models that describe this shape are called Power-Law processes, and they are based on D.B. Leeson's model of feedback oscillators (Leeson 1965). The models make use of classical feedback theory and consist of an amplifier with a noise figure, and a resonator in the feedback loop.

Noise in Amplifiers

Two sources of noise in junction transistors are thermal and shot noise. Thermal noise is generated in the base resistance and is due to the random motion of charge carriers. The mean-square noise voltage is given by

$$V_n^2 = 4KTRB$$

where K is Boltzman's constant (1.38×10^{-23} J/°k)

T is the temperature of the resistor R in kelvins

B is the bandwidth used, in Hz, for the measurement

Shot noise is generated at the diode junctions because the charge carriers that make up the diode current are randomly emitted from the collector, or emitter. Shot noise has also a flat spectral distribution, and it is given by

$$i_n^2 = 2qIB$$

where q is the electron charge.

Another noise called flicker, or f^{-1} , shows at the low frequencies and is caused by the surface recombination of minority carriers in the emitter-base depletion region (Krauss et al. 1980). This flicker characteristic is experimentally described by a corner frequency f_c , see Figure 28.

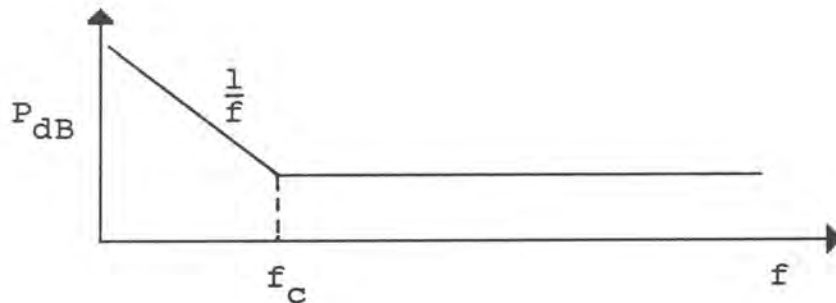


Figure 28. Amplifier noise spectrum.

In order to model an amplifier with a noise figure F , and a gain G the signal to noise ratio (SNR) at the input is divided by the SNR at the output

$$F = \frac{(S/N)_i}{(S/N)_o} = \frac{(S_i/N_i)}{(S_i G/N_o)} = \frac{N_o}{GN_i}$$

$$N_o = FGN_i$$

The maximum power that can be drawn from a source, using the maximum power transfer theorem, yields

$$N_i = \frac{V_n^2}{4R} = KTB$$

that is,

$$N_o = FGKTB$$

Since a 1 Hz bandwidth will be used, and the gain of the amplifier is 1 when oscillating

$$N_o = FKT$$

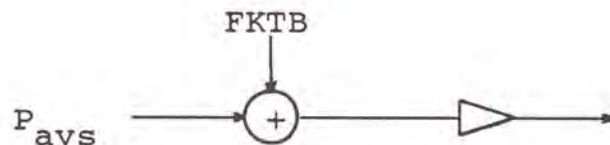


Figure 29. Model for a noise-free amplifier.

The simple model shown in Figure 29 needs to be modified to account for phase noise. Figure 30 shows how phase noise is added to a signal ($V_{RMS} = \sqrt{P_{avs}}$) passing through an amplifier with an equivalent noise voltage ($V_{nRMS} = \sqrt{FKT}$) at a frequency $f_o + f_m$.

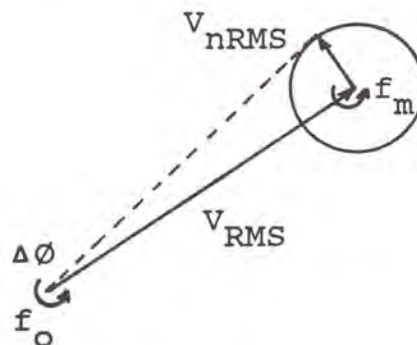


Figure 30. Phase deviation at $f_o + f_m$.

From Figure 30

$$\Delta\phi_P = \frac{V_{nRMS}}{V_{RMS}} = \sqrt{\frac{FKT}{P_{avs}}}$$

Adding, powerwise, the signal at $f_0 - f_m$

$$\Delta\phi_{RMS T} = \sqrt{\frac{FKT}{P_{avs}}}$$

using equation 3.1

$$S_\phi(f_m) = \frac{FKT}{P_{avs}} \quad (7.1)$$

Figure 31 shows the modifications made to figures 28 and 29 to account for phase noise. Equation 7.1 will also have to be modified to take into consideration the flicker characteristic.

$$S_\phi(f_m) = \frac{FKTB}{P_{avs}} \left(1 + \frac{f_c}{f_m}\right) \quad (7.2)$$

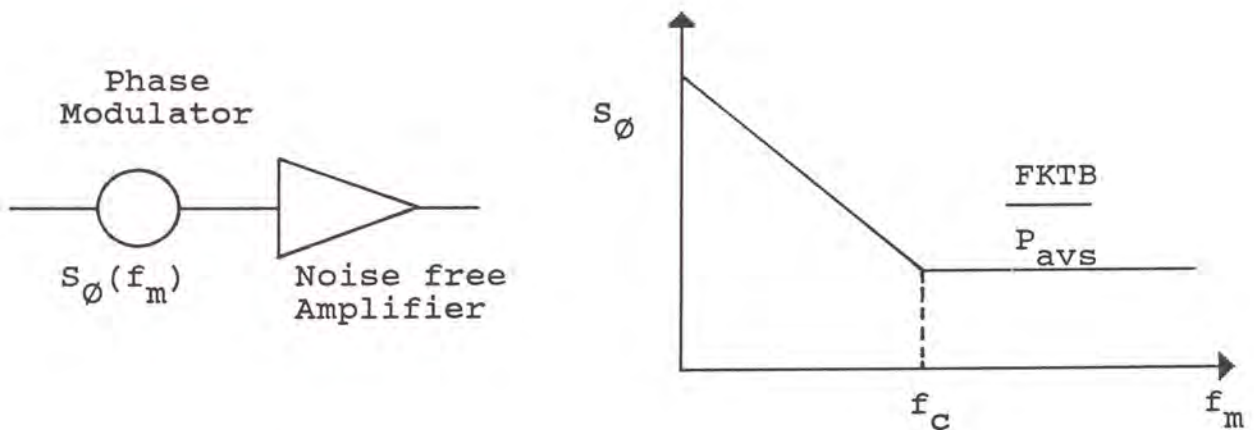


Figure 31. Amplifier's phase noise model.

Feedback Model of Phase Noise

The final model combining the phase noise model of the amplifier, and a resonator in the feedback loop can now be combined and analyzed (see Figure 32).

The resonator or bandpass filter transfers the phase modulation without attenuation up to rates equal to one-half its bandwidth, and attenuates the larger modulation rates. Instead of a bandpass transfer function an equivalent low-pass function will be used. The half bandwidth of the resonator is

$$\frac{\omega_o}{2Q_L}$$

and the low-pass transfer function is given by

$$\begin{aligned} L(f_m) &= \frac{1}{1 + j \frac{f_m}{f_{3dB}}} \\ &= \frac{1}{1 + j2Q_L \frac{f_m}{f_o}} \end{aligned} \tag{7.3}$$

Equation 7.3 is also the open loop gain.

The closed loop transfer function is given by

$$\frac{\Delta \phi_o}{\Delta \phi_i} = \frac{1}{1 - \frac{1}{1 + j2Q_L \frac{f_m}{f_o}}}$$

$$\frac{\Delta\phi_o}{\Delta\phi_i} = 1 + \frac{f_o}{j2Q_L f_m}$$

$$\Delta\phi_o(f_m) = \left(1 + \frac{f_o}{j2Q_L f_m}\right) \Delta\phi_i(f_m)$$

$$S_{\phi_o}(f_m) = \left[1 + \left(\frac{f_o}{f_m 2Q_L}\right)^2\right] S_{\phi_i}(f_m)$$

$$\mathfrak{f}(f_m) = \frac{1}{2} \left[1 + \frac{1}{f_m^2} \left(\frac{f_o}{2Q_L}\right)^2\right] S_{\phi_i}(f_m) \quad (7.4)$$

Equation 7.4 shows that the phase noise due to the amplifier alone, S_{ϕ_i} , is increased in the feedback loop by the quantity

$$\left[1 + \frac{1}{f_m^2} \left(\frac{f_o}{2Q_L}\right)^2\right]$$

Substituting equation 7.2 in 7.4

$$\mathfrak{f}(f_m) = \frac{FKTB}{2P_{avs}} \left[1 + \left(\frac{f_o}{f_m 2Q_L}\right)^2\right] \left(1 + \frac{f_c}{f_m}\right) \quad (7.5)$$

$$\mathfrak{f}(f_m) = \frac{FKTB}{2P_{avs}} \left[\frac{f_c}{f_m^3} \left(\frac{f_o^2}{2Q_L}\right)^2 + \frac{1}{f_m^2} \left(\frac{f_o}{2Q_L}\right)^2 + \frac{f_c}{f_m} + 1\right] \quad (7.6)$$

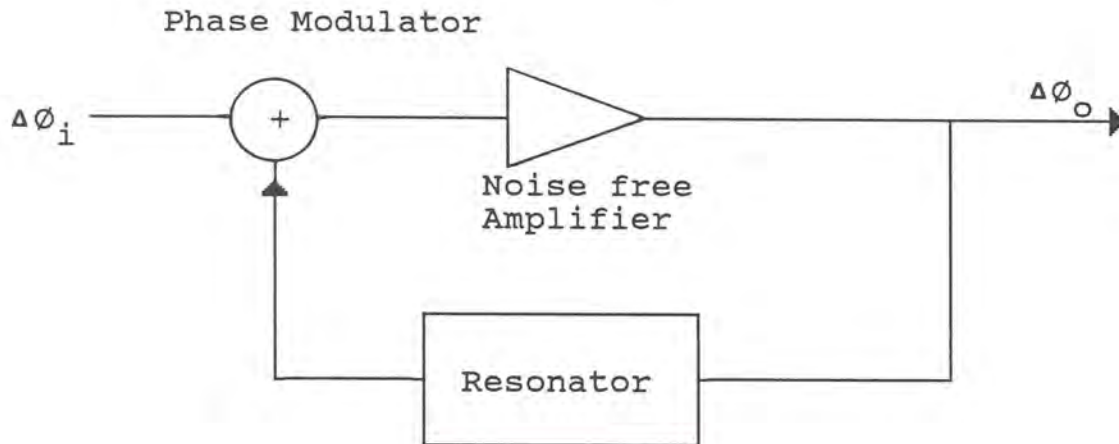


Figure 32. Phase noise feedback model.

PHASE NOISE DESIGN CONSIDERATIONS

The power-law process, or slope of a precision oscillator in the spectral density graph, is given in equation 7.6. This process is characterized by the dependence on the f_m frequency, and receives the following names (NBS Technical Note 679):

- f^0 = White phase noise
- f^{-1} = Flicker phase noise
- f^{-2} = White frequency noise
- f^{-3} = flicker frequency noise

Although it is possible to have all these processes, usually, there are only two or three present or dominant. Depending on the relationship of the corner frequency, f_c , and the half bandwidth of the resonator, equation 7.6 can be plotted two different ways (Vendelin 1982), as in Figure 33.

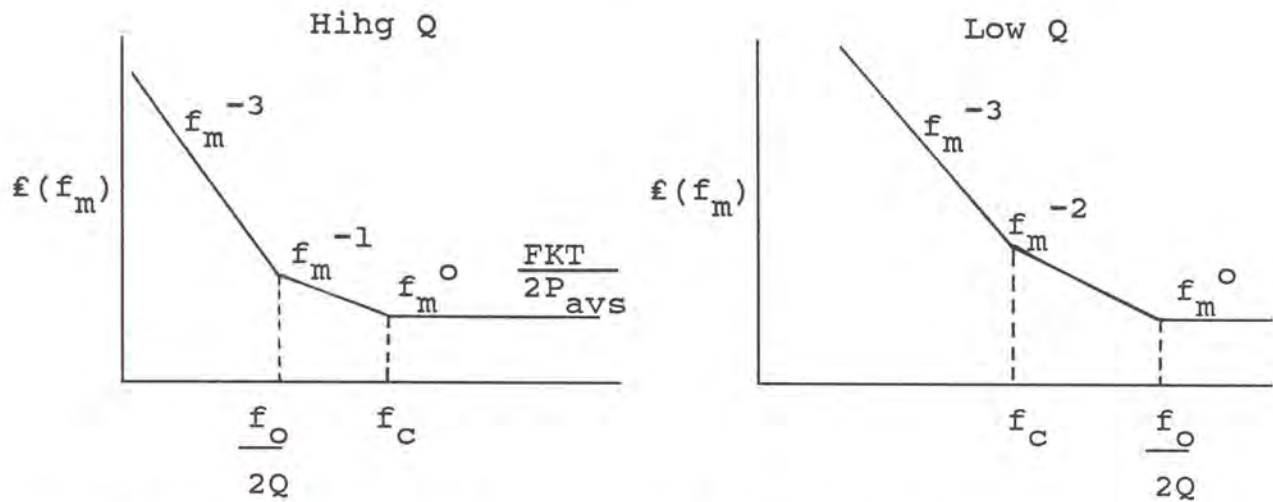


Figure 33. Power-law processes of oscillator phase noise.

From equation 7.5, for large f_m ($f_m \gg \frac{f_o}{2Q_L}$)

$$\epsilon(f_m) = \frac{FKTB}{2P_{avs}} \quad (7.7)$$

Equation 7.7 represents the thermal noise, or the theoretical minimum value the phase noise can have. It can be seen that the Q of the resonator does not affect this noise. This is expected since at frequencies much larger than the passband the feedback becomes unimportant due to its small magnitude. This minimum value can be calculated prior to the oscillator design. For example, using a noise figure (F) of 5 dB, a P_{avs} of 5 dBm, assuming room temperature ($T = 295 \text{ }^\circ\text{K}$), and a bandwidth of 1 Hz

$$\epsilon(f_m) = 10 \text{ Log}(KTB) + 5 \text{ dB} - 5 \text{ dBm} - 3 \text{ dB} = -176 \text{ dBm}$$

When f_m is within the half bandwidth the feedback has an important effect, and it is here that the Q can play an

important role in the design of a clean oscillator. Equation 7.5 and Figure 33 show that the higher the Q the smaller the phase noise. This is the single most important criteria in the design of a low phase noise oscillator. In order to have a starting point in the design, that of selecting the Q factor of the resonator, a first order approximation of equation 7.5 will be made for $f_m \ll \frac{f_o}{2Q_L}$

$$\mathfrak{f}(f_m) \approx \frac{FKT}{2P_{avs}} \left(\frac{f_o}{f_m 2Q_L} \right)^2 \quad (7.8)$$

Using this approximation the design process could start by calculating the necessary Q_L to obtain the specified $\mathfrak{f}(f_m)$ close to the carrier:

$$Q_L = \frac{f_o}{2f_m} \sqrt{\frac{FKT}{2P_{avs} \mathfrak{f}(f_m)_{req}}}$$

Other design considerations that can be extracted from equation 7.5 are: Choose an amplifier with not only a low noise figure, but also a low flicker noise. Select P_{avs} as large as possible within circuit constraints. Do not select the operating frequency higher than necessary; the higher the f_o the higher the phase noise.

CHAPTER EIGHT

CONCLUSION

After an introduction to the concepts of phase noise and spectral densities, this thesis concentrated in the design of a 100 MHz oscillator, and on phase noise measurements.

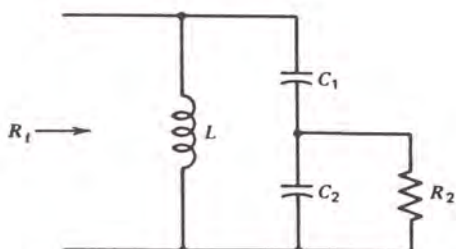
A second oscillator was built, with similar results, to prove the validity of the design procedure given. A word of caution: inductors with a low parallel resistance did not generate the oscillations, hence high Q inductors are recommended.

A new phase-locked loop technique was introduced and tested. The results were compared to measurements taken using the direct RF technique. This comparison showed that measurement range is gained by suppressing the carrier and translating the RF measurement to baseband. Further study is needed to compare this PLL technique to the Phase Quadrature Detection, and Frequency Discriminator techniques. Since these two techniques are implemented in complete systems such as the HP 11729C Phase Noise Test System, see Appendix C, another study on the potential of the PLL technique to be implemented as a phase noise test system would be needed.

APPENDICES

APPENDIX A
 OSCILLATOR DESIGN FORMULAS
 (Krauss et al. 1980)

COLPITT'S TANK CIRCUIT



For $Q_t \approx f_o/B \geq 10$,

(1) $C \approx 1/2\pi BR_t$

(2) $L \approx 1/\omega_o^2 C$

(3) $Q_t \approx f_o/B$

(4) $N = (R_t/R_2)^{1/2}$

(5) $Q_t/N \approx Q_p$. If $Q_t/N \geq 10$, use this value for Q_p and follow the formulas in the left-hand column. If $Q_t/N < 10$, follow the formulas in the right-hand column.

Approximate Formulas

$Q_p \geq 10$

Formulas for $Q_p < 10$

(6) $Q_p = \frac{Q_t}{N}$

(7) $C_2 = NC$

(8) $C_1 = \frac{C_2}{N-1}$

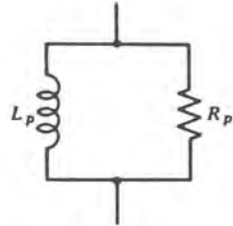
(6) $Q_p = \left(\frac{Q_t^2 + 1}{N^2} - 1 \right)^{1/2}$

(7) $C_2 = \frac{Q_p}{\omega_o R_2}$

(8) $C_{so} = \frac{C_2(Q_p^2 + 1)}{Q_p^2}$

(9) $C_1 = \frac{C_{so}C}{C_{so} - C}$

INDUCTOR SERIES-PARALLEL CONVERSION FORMULAS



Define: $X_p = \omega L_p$
 $Q_p = \frac{R_p}{X_p}$

Define: $X_s = \omega L_s$
 $Q_s = \frac{X_s}{R_s}$

*Parallel Equivalent of
the Series Network*

*Series Equivalent of
the Parallel Network*

EXACT FORMULAS

$$R_{pe} = R_s(1 + Q_s^2)$$

$$R_{se} = \frac{R_p}{1 + Q_p^2}$$

$$X_{pe} = X_s \left(\frac{Q_s^2 + 1}{Q_s^2} \right)$$

$$X_{se} = X_p \left(\frac{Q_p^2}{Q_p^2 + 1} \right)$$

$$L_{pe} = L_s \left(\frac{Q_s^2 + 1}{Q_s^2} \right)$$

$$L_{se} = L_p \left(\frac{Q_p^2}{Q_p^2 + 1} \right)$$

APPROXIMATE FORMULAS

If $Q_s \geq 10$

If $Q_p \geq 10$

$$R_{pe} \approx R_s Q_s^2$$

$$R_{se} \approx \frac{R_p}{Q_p^2}$$

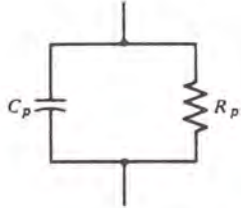
$$X_{pe} \approx X_s$$

$$X_{se} \approx X_p$$

$$L_{pe} \approx L_s$$

$$L_{se} \approx L_p$$

CAPACITOR SERIES-PARALLEL CONVERSION FORMULAS



Define: $X_p = \frac{1}{\omega C_p}$
 $Q_p = \frac{R_p}{X_p}$

Define: $X_s = \frac{1}{\omega C_s}$
 $Q_s = \frac{X_s}{R_s}$

*Parallel Equivalent of
the Series Network*

*Series Equivalent of
the Parallel Network*

EXACT FORMULAS

$$R_{pe} = R_s(1 + Q_s^2)$$

$$R_{se} = \frac{R_p}{1 + Q_p^2}$$

$$X_{pe} = X_s \left(\frac{Q_s^2 + 1}{Q_s^2} \right)$$

$$X_{se} = X_p \left(\frac{Q_p^2}{Q_p^2 + 1} \right)$$

$$C_{pe} = C_s \left(\frac{Q_s^2}{Q_s^2 + 1} \right)$$

$$C_{se} = C_p \left(\frac{Q_p^2 + 1}{Q_p^2} \right)$$

APPROXIMATE FORMULAS

If $Q_s \geq 10$

If $Q_p \geq 10$

$$R_{pe} \approx R_s Q_s^2$$

$$R_{se} \approx \frac{R_p}{Q_p^2}$$

$$X_{pe} \approx X_s$$

$$X_{se} \approx X_p$$

$$C_{pe} \approx C_s$$

$$C_{se} \approx C_p$$

APPENDIX B
PROGRAMS LISTINGS

"Numerical Integration," this basic program does a numerical integration of the function in line 50.

```
10 REM NUMERICAL INTEGRATION
20 LT=LOG(10)
30 INPUT "NN=?";NN
40 FOR I=0.000001 TO 10 STEP 1/NN
50 M=LOG(I)*I*EXP(-I*I/2)
60 M=M+MM
70 NEXT I
80 MM=MM/NN
90 LPRINT MM
```

5.797972E-02

"CL," this program, written for the Hewlett-Packard hand-held programable calculator 41-CV, prompts for the frequency of operation, and magnitude and phase of the element being measured. If the reactance is negative, the value of the capacitor will be displayed. If the reactance is positive, the value of the inductor will be given along with the value of its equivalent parallel resistance.

```
01 LBL "CL"
02 "W=?"
03 PROMPT
04 STO 03
05 "PHASE=?"
06 PROMPT
07 STO 01
08 "MAG=?"
09 PROMPT
10 STO 02
11 P-R
12 50
13 *
```



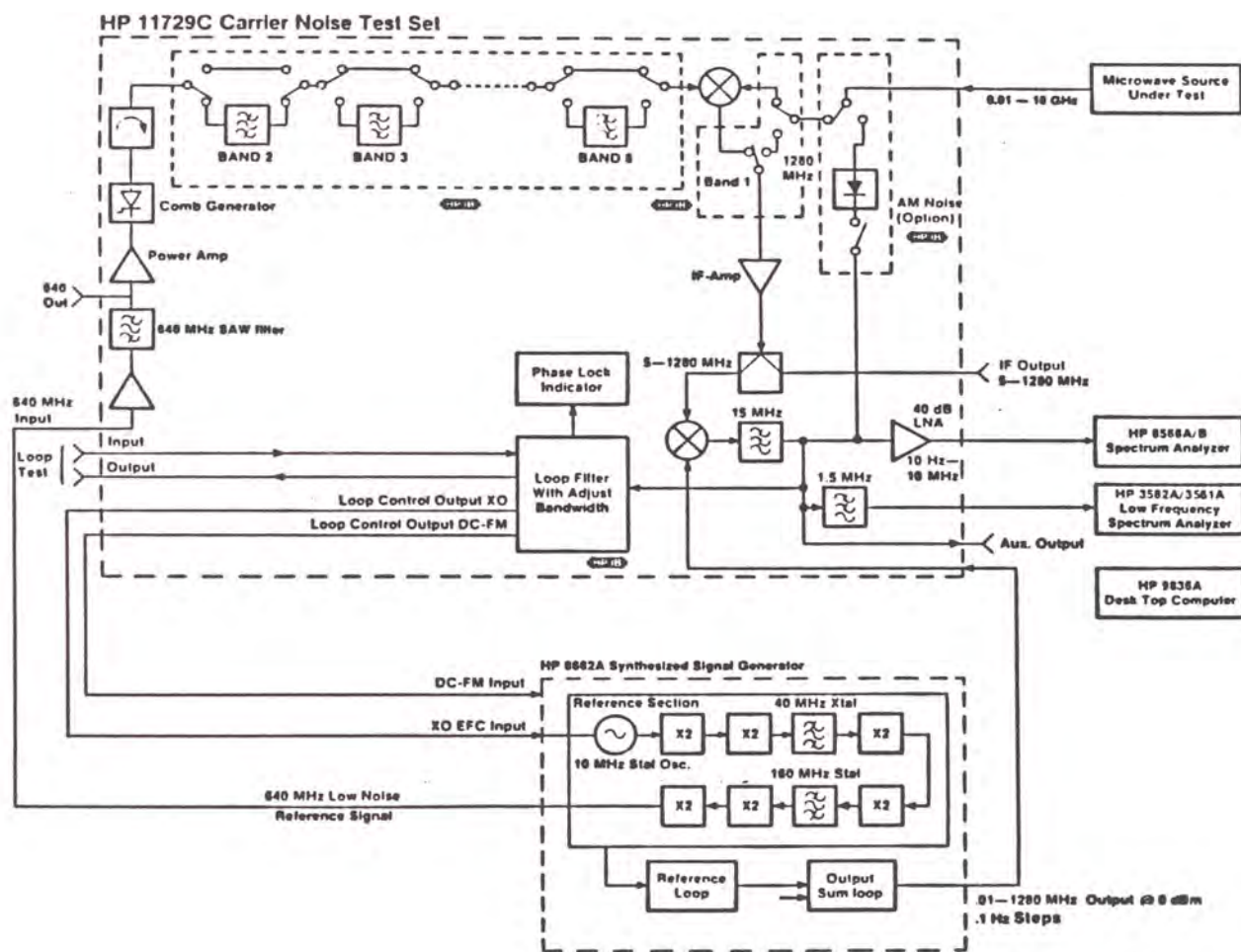
```
14 STO 04
15 X<>Y
16 50
17 *
18 STO 05
19 0
20 X<>Y
21 X>Y?
22 GTO 01
23 RCL 03
24 *
25 CHS
26 1/X
27 STO 06
28 "C="
29 ARCL X
30 AVIEW
31 STOP
32 LBL 01
33 RCL 03
34 /
35 STO 07
36 "L="
37 ARCL X
38 AVIEW
39 STOP
40 RCL 05
41 RCL 04
42 /
43 STO 08
44 X^2
45 1
46 +
47 RCL 04
48 *
49 STO 09
50 "RP="
51 ARCL X
52 AVIEW
53 END
```

"SØ," this program prompts for dBV, and the offset frequency fm. Converts dBV to Vrms, and solves equation 6.2. Finally, it subtracts 3 dB to convert SØ to £(fm).

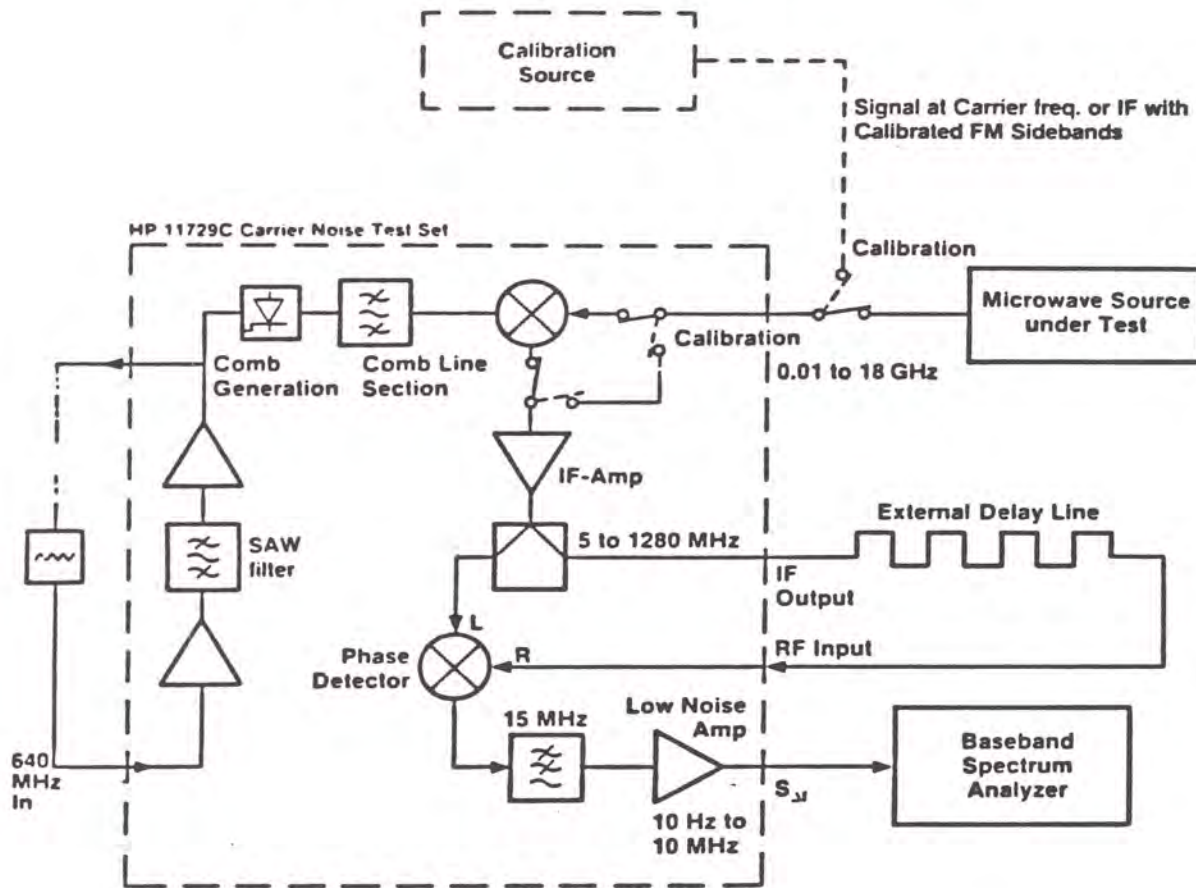
```
01 LBL "SØ"
02 "dBV=?"
03 PROMPT
04 STO 01
05 "fm=?"
06 PROMPT
07 STO 03
08 RCL 01
09 20
10 /
11 10^X
12 8.91*10-6
13 X^2
14 RCL 03
15 X^2
16 *
17 4
18 *
19 PI
20 X^2
21 *
22 /
23 LOG
24 10
25 *
26 3
27 -
28 "£(fm) ="
29 ARCL X
30 AVIEW
31 END
```

APPENDIX C

PHASE NOISE TEST SYSTEMS (Scherer 1986)



HP 11729C Operating in Discriminator Mode

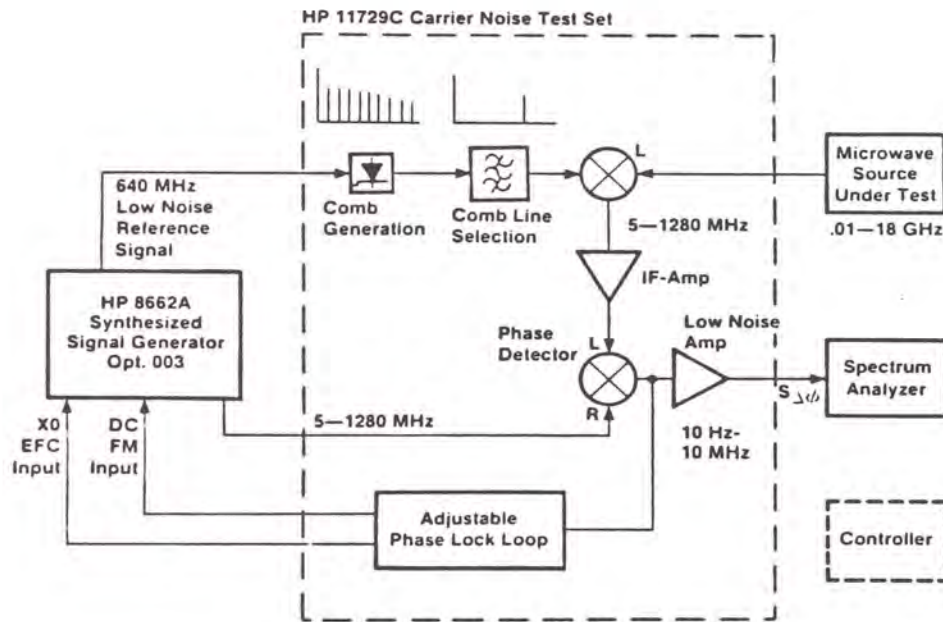


- Low noise down conversion of microwave signal under test
- Delay line operating at IF (5—1500 MHz)
- Calibration signal provided by HP 8662A
- Phase quadrature indication.

The HP 11729C may also be used in a delay line discriminator mode. The microwave reference signal generated by the 640 MHz signal down converts the source under test into the IF range. The power splitter and auxiliary IF output allows one to simply insert an appropriate delay line externally.

Delaying the signal at IF means lower delay line losses and also a wider choice of delay devices, like e.g. SAW delay line. Any signal generator with FM sidebands at IF or RF can serve as a calibration tool.

HP 11729C/8662A Phase Noise Test System Principle of Operation (Phase Detector Method)

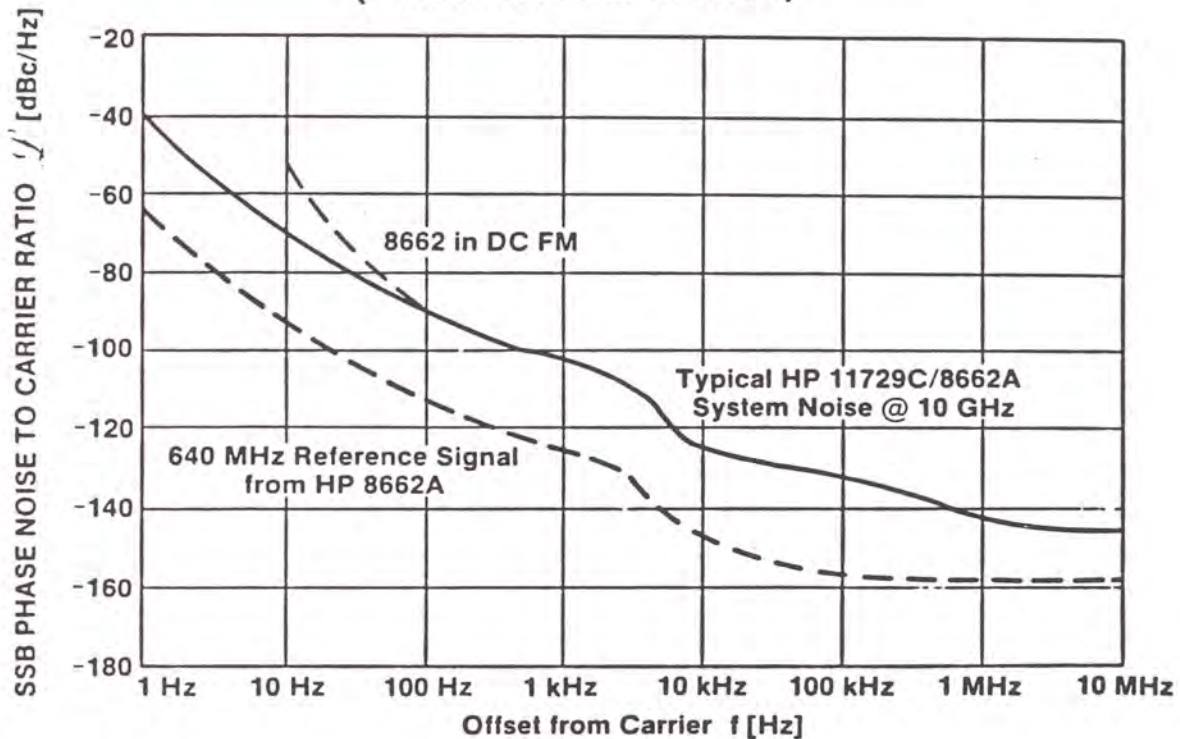


The HP 8662A Synthesized Signal Generator provides a state-of-the-art low noise reference signal at 640 MHz to the HP 11729C Carrier Noise Test Set. This signal is applied to a step recovery diode multiplier which generates a comb of signals spaced by 640 MHz ranging beyond 18 GHz. A switched in filter selects an appropriate combline. This microwave reference signal down converts the microwave source under test into an IF range of 5 to 1280 MHz.

The double balanced mixer phase compares the IF signal with the output signal of the HP 8662A (.01 to 1280 MHz). Phase quadrature is enforced by phase locking the HP 8662A to the signal under test either thru the limited electronic control of the HP 8662A's 10 MHz crystal oscillator or thru its DC-FM port. The loop bandwidths can be set over a 4 decade range.

A first order phase lock loop is enabled by the capture feature making lock acquisition easy. Then the second order phase lock loop (with very high dc gain) maintains lock and phase quadrature. To enable phase noise measurements within the loop bandwidth, the phase noise suppression can be characterized via the loop test ports.

Noise Floor of HP 11729C/8662A Phase Noise Test System (Phase Detector Method)



$$L_{\text{system}} = 10 \log (N^2 \times 10^{\frac{K_1}{10}} + 10^{\frac{K_2}{10}} + 10^{\frac{K_3}{10}})$$

N Multiplication number of the 640 MHz signal

K_1 Absolute SSB Phase Noise of the 640 MHz reference signal (dBc/Hz).

K_2 Absolute SSB Phase Noise of the 5 to 640 (1280) MHz tunable signal (dBc/Hz).

K_3 Two-port noise of HP 11729C (dBc/Hz).

Offset from carrier	Typical 640 MHz low noise output	Typical 320-640 MHz tunable 8662A output	Typical Two-port noise of HP 11729C @ 5 GHz	Typical Two-port noise of HP 11729C @ 10 GHz
1 Hz	-64 dBc	-64 dBc	-99 dBc	-93 dBc
10 Hz	-94 dBc	-94 dBc	-112 dBc	-106 dBc
100 Hz	-114 dBc	-114 dBc	-125 dBc	-119 dBc
1 kHz	-126 dBc	-125 dBc	-132 dBc	-126 dBc
10 kHz	-149 dBc	-136 dBc	-137 dBc	-131 dBc
100 kHz	-159 dBc	-136 dBc	-148 dBc	-142 dBc
1 MHz	-159 dBc	-146 dBc	-153 dBc	-147 dBc

For most microwave applications, K_1 , the SSB phase noise of the 640 MHz reference signal, is the dominating factor in setting the noise floor of the system as its phase noise is multiplied up to microwave frequencies.

REFERENCES

- Howe, D.A. "Frequency Domain Stability Measurements: A Tutorial Introduction." NBS Technical Note 679. (March 1976): p. 2.
- Krauss, Herbert L.; Bostian, Charles W.; and Raab, Fredrick. Solid State Radio Engineering. New York: John Wiley and Sons, 1980.
- Leeson, D.B. "A Simple Model of Feedback Oscillator Noise Spectrum." Proceedings IEEE. 54 (Feb. 1966): p. 329
- Moulton, G. "Dig for the Roots of Oscillator Noise." Microwaves & RF. 25 (April 1986): p. 65.
- Phase-Locked Loop Data Book. Sunnyvale, CA.: Exar, 1979.
- Reference Data for Radio Engineers. 4Ed. New York: ITT, 1956: p. 991.
- Scherer, D. "Recent Advances in the 'Art' of Phase Noise Measurements." RF & Microwave Measurement Symposium and Exhibition. Hewlett-Packard, February 1986.
- "Spectrum Analysis Noise Measurements." Hewlett-Packard Application Note 154, April 1974.
- Vendelin, George D. Design of Amplifiers and Oscillators by the S-Parameter Method. New York: McGraw-Hill Book Company, 1982.
- Ziemer, R.E., and Tranter W.H. Principles of Communications. Boston: Houghton Mifflin Company, 1985.